neel.cnrs.fr

HIGHLIGHTS 2012

NÉEL institut

EDITORIAL

In this issue of "Highlights" magazine, our aim is to illustrate the wealth and diversity of the research work carried out at the NEEL Institute. It would be impossible to detail all the results obtained by a laboratory that produces more than 400 scientific publications each year. Hence, we have collected 17 articles representing a selection of research themes that culminated in particularly significant scientific or technical advances during the past year.


Alain BENOIT


Benoit BOULANGER


Joël CIBERT

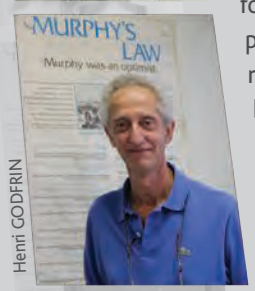

Henri GODFRIN


Ioan POP

While focussing attention on the most exceptional results, we must recall that the overall quality of the research conducted in a large laboratory like the NEEL Institute is the result of the combined creativity and hard work of all its personnel: researchers, university faculty, engineers, technicians and administrative staff. The Institute's outstanding research productivity draws on the cooperation between its individual research teams, on sharing expertise, means and equipment within the laboratory. Of comparable importance is our strong position within the greater Grenoble scientific community, especially the relations with our neighbour laboratories in the framework of the Nanosciences Foundation and the LANEF Project.

Again this year, NEEL Institute researchers have received numerous prizes and distinctions for their work. Amongst the most prestigious, we mention the following: the Y. Rocard prize for Technology Transfer was accorded by the French Physical Society to Patricia De Rango, Daniel Fruchart and Salvatore Miraglia together with Philippe Marty of the LEGI laboratory (Grenoble) and Michel Jehan of the technology company McPHY Energy; Joël Cibert received the Academy of Sciences *grand prix* France Telecom; the Innovation Medal of the CNRS was presented to Alain Benoît by Research Minister Geneviève Fioraso; the French Physical Society's *Prix Spécial* was awarded to Wolfgang Wernsdorfer; Benoît Boulanger has been named a Fellow of the European Optical Society; and Ioan Pop won the Nanosciences Foundation prize for best Ph.D. thesis. Details of the work done by these researchers can be found on our website *neel.cnrs.fr*.

Building on the long experience of its founding laboratories, the NEEL Institute has now been in existence for five years, five years during which initiatives taken have yielded excellent results including those presented here. In 2012, we have taken the opportunity to reassess this initial period, with a view to refining our modes of operation. The first *"Journées NEEL"* event — an internal two-day seminar that brought together 300 staff members— was an exceptional moment in this phase of evaluation and proposal.

To-day's projects will lead to the results of tomorrow. Certain new projects have already received special recognition, from the European Research Council. The ERC "Starting Grants" assist the most brilliant young European researchers to undertake challenging research projects. We are particularly proud to count four young NEEL Institute researchers — Wiebke Guichard, Olivier Arcizet, Jacek Kasprzak and Tristan Meunier —among the laureates of these European grants. This issue of "Highlights" contains short summaries of the motivation and objectives of their research projects.

The coming year will see the opening of our new building, designed principally for research in the nanosciences and to house experimental apparatus requiring a very low noise environment. I am confident that this new facility, a direct product of the commitment of the Institute's founders, will enable our researchers to further develop research of the highest quality at the NEEL Institute.


Patricia DE RANGO Daniel FRUCHART Salvatore MIRAGLIA

Alain SCHUHL
Director of NEEL Institute, CNRS-UJF

CONTENTS

DIRECTOR OF PUBLICATION
Alain SCHUHL

EDITORS
Signe SEIDELIN, Ronald COX

LAYOUT - PRODUCTION
Nathalie BOURGEAT-LAMI, Quentin RICHARD

COVER
SYNTHESE ECA

PRINTING
PressVercors

DATE OF PUBLICATION : 2012

Table-top dilution cryostat: Sionludi

A series of table-top dilution cryostats has been realized at the Néel Institute. These cryostats, which are highly appreciated by our experimentalists, make it possible to reach temperatures of about 30 mK in only 3 hours. The currently available cooling power is about 200 µW at 100 mK and the minimum temperature is about 15 mK.

Dilution cryostats achieve very low temperatures by diluting liquid He^3 in liquid He^4. The mixing process is endothermic, thus extracting heat from the surroundings. This allows cooling of experimental samples or devices to very low temperatures. Our new, improved dilution cryostats (see Figure) were developed by the cryogenic, experimental, and mechanical engineering teams of the Néel Institute, inspired by the design of the "upside-down" dilution refrigerator called ''Sionludi'', which was invented by A. Benoit in 1990. 20 years of user-experience allowed us to improve the performance as follows:

- two times faster cooling
- 4 times higher cooling power
- 4 times lower temperatures
- reduced liquid He consumption (less than 8 litres/day).

New generation of the Sionludi table-top dilution cryostat, with its thermal shields and outer vacuum container removed. The compact, inverted design allows the cryostat to be mounted on a bench top. The sample space is located on top of the upper plate, making it easily accessible.

These improvements were achieved by optimizing the injection and pumping lines, mixing chamber, cold mass, and by an improved geometry. We also rearranged the elements in the system in order to maximize the space available for each cooling stage.

Our dilution cryostats are composed of a vacuum chamber containing a succession of six cryogenic stages whose temperatures progress down from 80 K to 15 mK. In order to increase the efficiency, each stage - consisting of a plate and a thermal shield - is situated inside the following stage, going from very low to higher temperatures, analogous to a Russian doll.

The outer two stages, at 80 and 20 K, are cooled by means of a counter-flow heat exchanger, in which we find the He^3/He^4 injection lines and the He^4 pumping line. The third stage at 4 K is permanently cooled from a liquid He^4 storage vessel located directly under the cryostat. This stage can also be used to cool heavy experimental parts close to the sample, such as superconducting field coils.

The fourth stage at 0.8 K is thermalized to the so-called "still". The still continuously extracts the He^3 from the mixture, thus allowing a steady-state operation. The fifth stage at 50 mK can absorb a heat load of about 1 mW. The last stage is the mixing-chamber stage with a base temperature of about 15 mK. These last three stages represent the heart of the dilution refrigerator where only the He^3/He^4 mixture circulates. They contain a Joule-Thomson heat exchanger, which replaces the "1-K-box" of a classical dilution system. It also contains the condensation impedance, the still, a counter-flow heat exchanger, several discrete heat exchangers, and the mixing chamber.

This device has received an increasing interest for users because of the following principal advantages:

Greatly improved accessibility of the cold volume: Contrary to traditional dilution refrigerators, the coldest part of the cryostat is easily accessible. This cold volume is situated at the top of the apparatus, separated from the 300 K vacuum chamber only by 3 to 5 thermal shields. This is an unquestionable advantage for rapid sample-changing and for direct optical or mechanical access.

Compactness and rigidity: The mechanical structure of the Sionludi design makes it compact and rigid, which allows us to achieve a high level of stability. For example, it can be used for cooling STMs (Scanning Tunneling Microscopes) and AFMs (Atomic Force Microscopes) and generally for all experiments that require a low level of vibration.

Considerably improved performance: The time needed to reach the target temperature is a prime factor for experimentalists. This device - designed with fast and slow injection lines, associated with the compactness of these lines - makes it possible to reach low temperatures in only 3 hours. Moreover, a fast circulation of the He^3 allows us to reach a high cooling power of 200 µW. Finally, without being completely optimized, the volume of He^3 needed for the He^3/He^4 mixture remains relatively low (7 litres of gaseous He^3).

A new version of this dilution cryostat is under construction. It will integrate a top-loading system, which will allow the transfer of samples between an ultra-high vacuum chamber and the precooled table-top dilution cryostat.

CONTACTS
Guillaume DONNIER-VALENTIN
gdonnier@grenoble.cnrs.fr
Wolfgang WERNSDORFER
wolfgang.wernsdorfer@grenoble.cnrs.fr

Optically dressed magnetic atoms

The continuing decrease of the size of the structures used in semiconductor electronics and in magnetic information-storage devices has dramatically reduced the number of atoms necessary to process and store one bit of information: An individual magnetic atom would represent the ultimate size limit for storing and processing information. Towards this goal, we have demonstrated that an individual manganese atom embedded in a semiconductor quantum dot may act as a spin-based memory. Further, a pair of Mn atoms can act as a prototype of a pair of coupled memory units. We can exploit the optical absorption and emission of the quantum dot in order to initialize and to read out the spin state of the magnetic atoms. Under resonant optical excitation, we can enter the "strong coupling" regime where hybrid states of matter and the electromagnetic field are created, and this could be used for a coherent, optical "manipulation" of the Mn spin.

In our research, the quantum dot is an island of the semiconducting compound CdTe inside a layer of ZnTe. Absorption of an incident photon creates an electron-hole pair (an "exciton") in the quantum dot, see Fig. 1. Inversely, a photon is emitted when the two carriers annihilate each other.

With a single Mn atom introduced in the dot, the energy and polarization of the photon emitted or absorbed by the dot depends on the spin state of the S=5/2 magnetic atom. This is due to the exchange interaction present in the excited state, between the confined electron-hole pair and the Mn spin. The exciton acts as an effective magnetic field, directed along the dot's growth axis z. This effective field splits the 2S+1=6 spin states of the Mn atom (which are almost degenerate in the absence of the exciton), leading to a 6 line optical spectrum for the quantum dot (e.g. Fig.2, top left).

We had already shown that laser excitation resonant with one of these optical transitions can be used to initialize a localized Mn spin and to probe its dynamics optically: The Mn atom behaves like an optically addressable long-lived spin-based memory. To go further, information processing using individual spins will require fast coherent control of a single spin and also tuning of the coupling between two or more spins. We recently achieved two important steps towards these challenging goals.

Concerning the latter objective, for quantum dots containing two Mn atoms (which give complex spectra with up to 6x6=36 lines, e.g. Fig 2 at top right), we have shown that the precessional motions of the Mn spins become correlated with each other under optical excitation, as a result of their mutual interaction with the carrier spins. This carrier-mediated interaction could be exploited in the future to optically control the coupling between two Mn spins. Next, we have demonstrated that under a strong resonant optical field, the energy of any given spin state of one Mn atom or of a pair of Mn atoms can be tuned using the optical Stark effect. The intensity maps of Fig. 2 illustrate this for the case of the dot containing a pair of Mn.

Under optical excitation exactly resonant with an absorption transition, we can enter the strong coupling regime where hybrid states of matter and light are created. The ground state of the magnetic atoms is "dressed" with light. The spin dependent strong coupling with the laser field modifies the Mn fine structure (interaction with the crystal field) and hyperfine structure (interaction with the ^{55}Mn nuclei). The optically controlled energy shift affects the spin dynamics of the magnetic atoms. It will be used in future experiments for a coherent optical manipulation of both the electronic and the nuclear spins of individual and coupled Mn atoms.

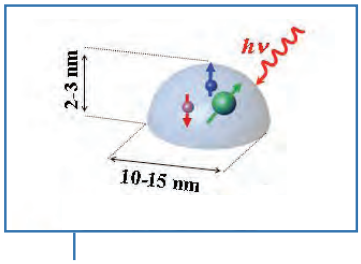

Figure 1: Illustration of a CdTe quantum dot containing an individual Mn atom (green) and an optically-created exciton (electron-hole pair).

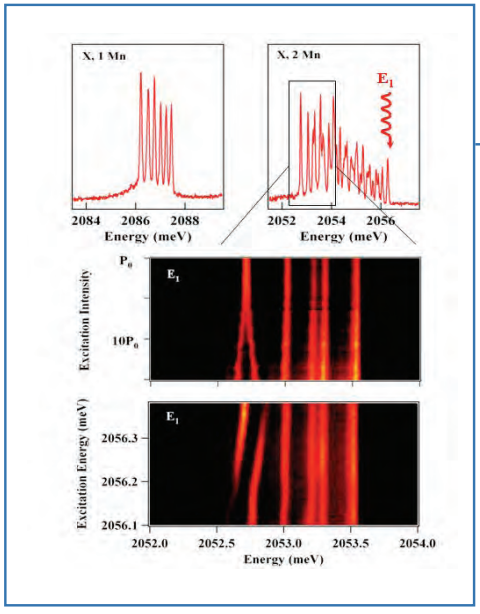

Figure 2: At top: Photoluminescence spectra (6 or 36 lines) resulting from the recombination of an exciton X in a CdTe quantum dot containing one Mn (left) or two Mn atoms (right). Below: Maps of photoluminescence intensity for the dot with two Mn atoms; a single mode laser excites the dot above the range shown. In the upper panel we vary the laser power (logarithmically) with the laser tuned to precise resonance with the highest energy excited state E_1 (spin state $|S_{z1}=S_{z2}=+5/2; J=+1>$) where S_{zi} and J are the angular momentum of Mn atom i and exciton respectively). In the lower panel, the laser is scanned through the energy E_1. One observes a power-dependent and tuning-dependent splitting of the recombination emission of the lowest energy excited state $|S_{z1}=S_{z2}=+5/2; J=-1>$. Since the ground state $|S_{z1}=S_{z2}=+5/2>$ is the same for both transitions, this shows that the Mn spins of the ground state are "dressed" by the resonant laser field.

CONTACTS

Lucien BESOMBES
lucien.besombes@grenoble.cnrs.fr

Hervé BOUKARI
herve.boukari@grenoble.cnrs.fr

Ph.D STUDENTS

Claire LE GALL

Chong Long CAO

FURTHER READING

OPTICAL INITIALIZATION, READOUT AND DYNAMICS OF A Mn SPIN IN A QUANTUM DOT
C. Le Gall, R. S. Kolodka, C. L. Cao, H. Boukari, H. Mariette, J. Fernández-Rossier and L. Besombes
Phys. Rev. B 81, 245315 (2010).

OPTICAL STARK EFFECT AND DRESSED EXCITON STATES IN A Mn DOPED QUANTUM DOT
C. Le Gall, A. Brunetti, H. Boukari and L. Besombes
Phys. Rev. Lett. 107, 057401 (2011).

Unified picture for diluted magnetic semiconductors

For more than a decade already and because of their technological potential for incorporation in spintronic devices, diluted magnetic semiconductors (DMS's) have attracted a considerable attention from both experimentalists and theoreticians. A very competitive race started with the discovery that a very small amount of Mn (which introduces a $3d^5$ configuration + itinerant hole) in thin films of the III-V semiconductor GaAs could lead to a relatively high Curie temperature ferromagnet. (Ga,Mn)As rapidly became the most studied prototype, which still exhibits (for a given Mn density and well annealed samples) the highest critical temperature among III-V DMS compounds (190 K). However, even today, from the physical understanding and theoretical point of view, one often finds contradicting theories and results in the literature.

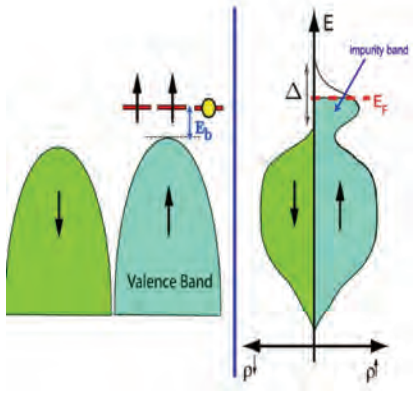

Figure 1: (Left) A single Mn in GaAs; the E_b = 113 meV p-d acceptor level is threefold degenerate. (Right) the spin resolved density of states for a finite Mn concentration in the ferromagnetic phase. Δ is the band splitting.

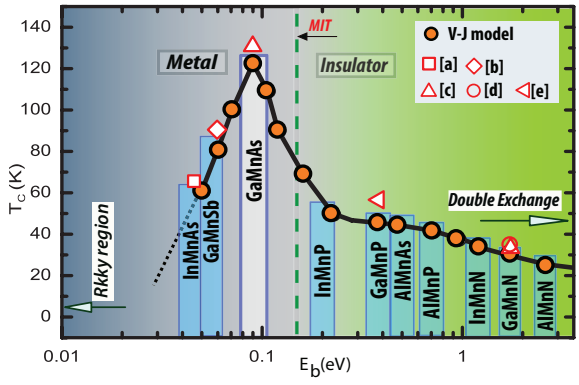

Figure 2: Curie temperature (in K) as a function of the p-d Mn acceptor level position E_b (eV) in various III-V semiconductors. The Mn density is x = 5%. Filled symbols are computed within the V-J model, open symbols (a,b,..e) with ab initio exchange integrals. The agreement between ab initio studies and V-J model calculations is excellent. A metal-insulator transition occurs at E_b=0.15 eV, close to (Ga,Mn)As.

CONTACTS

Richard BOUZERAR
richard.bouzerar@grenoble.cnrs.fr

Georges BOUZERAR
georges.bouzerar@grenoble.cnrs.fr

FURTHER READING

UNIFIED PICTURE FOR DILUTED MAGNETIC SEMICONDUCTORS
R. Bouzerar and G. Bouzerar
Europhys. Lett. 92, 47006 (2010).

FIRST PRINCIPLES THEORY OF DILUTE MAGNETIC SEMICONDUCTORS
K. Sato, G. Bouzerar, et al.
Rev. Mod. Phys. 82, 1633 (2010).

OPTICAL CONDUCTIVITY IN Mn DOPED GaAs
G. Bouzerar and R. Bouzerar
New J.Phys. 13, 023002 (2011).

Several crucial questions are still debated and very controversial. In spite of the great success of ab initio material-specific theory in providing accurate Curie temperatures (TC) in various III-V based materials, the ultimate search for a unifying theory was still an open issue. We have shown recently that a simple one-band model, namely the V-J model (where V is the spin independent scattering of the holes by Mn^{2+} and J is the p-d exchange between Mn d orbitals and host p-holes) is able to provide the missing unified picture and clarify numerous issues. Within this model we can understand and explain magnetic and transport properties simultaneously, not only qualitatively but also quantitatively. It has been shown that the position E_b of the Mn p-d hybridized acceptor level, with respect to the top of the valence band, is the key physical parameter (controlled by V). This term is the source of the crucial differences between II-VI and III-V Mn doped systems. It controls both the magnetic properties (nature of the couplings) and the transport properties. We obtain a very good agreement between the splitting of the valence band density of states as calculated by the model and that obtained from material-specific ab initio calculations. And our calculations agree very well with experimental measurements for optimally prepared samples of various III-V compounds.

The V-J model provides a coherent picture for the drastic change in the nature of the couplings depending on the host: RKKY-like (oscillating long range couplings) in II-VI compounds such as (Zn,Mn)Te, (Cd,Mn)Te and double exchange-like (very short range and ferromagnetic) in wide band gap compounds such as (Ga,Mn)N. It has also been possible to explain why, among all Mn doped materials either II-VI or III-V, the highest critical temperature was measured in (Ga,Mn)As. As seen in Fig.2, (Ga,Mn)As is precisely located on a peak where the Mn-Mn couplings are optimal. The V-J model also explains clearly why it has been observed experimentally that some as grown (Ga,Mn)As samples are insulating and others are metallic at low temperature, or why one can trigger an insulator to metal transition after annealing. Indeed, (Ga,Mn)As appears to be at the boundary of the Metal-Insulator Transition (MIT) as seen in Fig.2. As a further confirmation of the validity of our model, it has also been possible (i) to reproduce quantitatively the measured infrared conductivity and (ii) explain why annealing, which increases the hole density, induces a red shift of the conductivity peak located at about 200 meV.

Electrons surfing on a sound wave

Single-electron circuitry is a promising route for processing quantum information, but it requires a mechanism to transport single electrons from one functional part of the circuit to another. Until now, this has only been possible between quantum dots (small electronic islands that can contain as little as a single electron) if they are spaced extremely close to each other. However, when propelled by a sound wave, a single electron can be transferred between two distant quantum dots with very high fidelity. This opens new avenues in the field of quantum computing with electrons.

A single electron can be isolated in a small region of a two-dimensional electron gas that is sandwiched at the interface between two semiconductors GaAs and AlGaAs. To achieve this, negative voltages are applied to electrostatic gates deposited on the surface of the semiconductor (areas represented in magenta in Fig. 1). A sufficiently high voltage depletes the underlying region to the point where only a single electron remains trapped, within a so-called quantum dot formed by the electric field. In such structures, one can perform efficient quantum manipulations that operate on the spin of the electron.

To use the quantum properties of the electron spin in computation, an important requirement is to be able to interconnect distant quantum dots and to displace a single electron within a semiconductor chip in a controlled manner. However, for distances greater than a few hundred nanometers, this has remained a challenge. In a recent experiment, our research team at the Néel Institute has finally achieved this goal.

Working with colleagues from the University of Tokyo and the Ruhr University, Bochum (Germany), we have demonstrated that a single flying electron – an electron "surfing on a sound wave" - can be sent on demand from one quantum dot via a one dimensional quantum channel – the "quantum bus" – and re-trapped in a second quantum dot, after propagation, with very high efficiency.

The quantum bus consists of a several microns long region that is entirely depleted of electrons, within the two-dimensional electron gas. It is defined by the two large (grey-coloured) gate electrodes shown in Fig. 1. Initially, a single electron is trapped within the left quantum dot defined by the electrostatic gates highlighted in magenta. Utilizing the piezoelectric properties of GaAs, we can generate a sound wave that propagates at the surface of the chip. When we trigger the sound wave, the electron is literally expelled from the quantum dot, propelled through the quantum bus and captured in the second quantum dot.

With a sound velocity of approximately 3000 m/s this voyage takes only a few nanoseconds. Moreover, we have demonstrated that transfer of the electron could be launched on demand at a timescale smaller than the coherence time (the time over which phase information is lost) in GaAs spin "qubits" (quantum bits), an important ingredient necessary for the distant manipulation of qubits. Our demonstration of single-electron transfer between two distant quantum dots brings the technology a step closer to this goal.

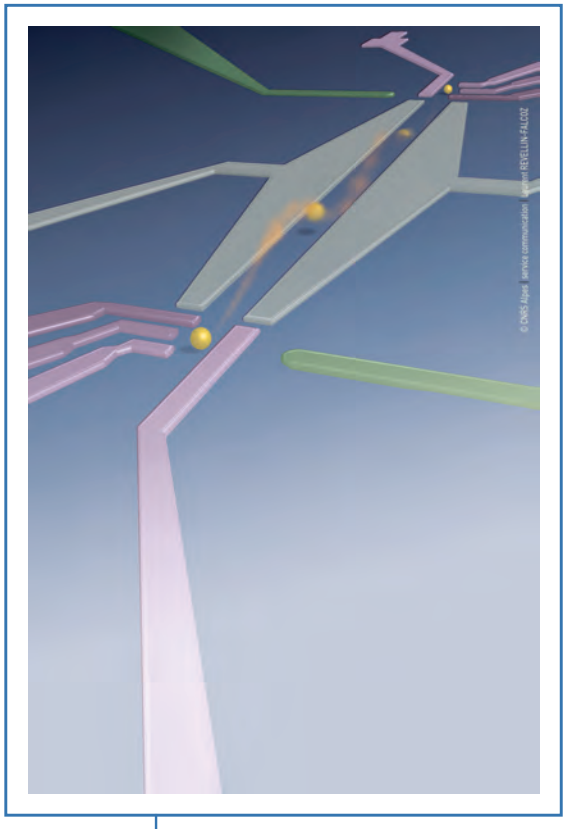

Artist's view of single electron transport between two distant quantum dots, assisted by a sound wave. The two quantum dots, defined by the electrostatic gates coloured in magenta, are interconnected by a long "quantum bus" (grey). A single electron, trapped initially in the left quantum dot, is propelled by a sound wave towards the second quantum dot, at distance 3 microns.

CONTACTS

Christopher BAUERLE
christopher.bauerle@grenoble.cnrs.fr

Tristan MEUNIER
tristan.meunier@grenoble.cnrs.fr

Ph.D STUDENT
Sylvain HERMELIN

FURTHER READING

ELECTRONS SURFING ON A SOUND WAVE AS A PLATFORM FOR QUANTUM OPTICS WITH FLYING ELECTRONS

S. Hermelin, S. Takada, M.Yamamoto, S. Tarucha, A. D. Wieck, L. Saminadayar, C. Bäuerle & T. Meunier
Nature 477, 435 (2011).

Efficient parametric amplification in a nano-electro-mechanical device

Parametric amplification is an extremely useful scheme applied in optics, electronics and also mechanics. In mechanics it occurs when a mechanical parameter of the oscillator (such as its spring constant) is modulated at twice the resonance frequency of the oscillator mode studied. We have recently achieved this type of amplification with an extremely small device, a silicon nano-electro-mechanical system (a NEMS).

Our structure resonates around 7 MHz. It consists of two "feet" (length l' ≈ 3 µm) linked by a "paddle" (l ≈ 7 µm), see top image in Fig. 1. It moves in the out-of-plane first flexural mode. The width and thickness of the three beams are about 200 nm.

We use the magnetomotive scheme to actuate and detect the motion of the paddle. An AC current is fed through the device thanks to a conducting metallic coating, which along with a static magnetic field generates a Laplace force, at frequency f_0=7 MHz. The 7 MHz motion in turn creates a voltage (Lenz's law), which is detected with a lock-in amplifier (referenced at f_0). The spring constant is modulated at $2f_0$ by a voltage applied on a strongly capacitively-coupled gate electrode (gap between electrode and NEMS g ≈ 100 nm). The electric field adds a strongly nonlinear restoring force which we use here to implement the parametric amplification scheme.

We use the Laplace force as our test force to be amplified by the parametric scheme. Depending on the relative phase between this force (i.e. the drive current at f_0) and the modulation of the spring constant (i.e. the gate voltage at $2f_0$), one can either amplify or "de-amplify" (squeeze) the vibration, see Fig. 2. ("Squeezing" means that a particular phase-component of the vibration is attenuated while the other component is unaffected).

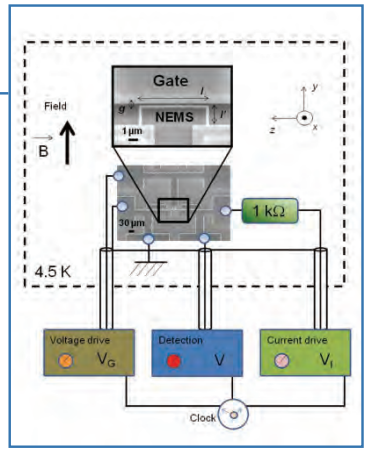

Figure 1: Sample and experimental setup. The device (see text for description) resonates at 7 MHz. A dual channel generator drives the mechanical vibrations at f_0= 7 MHz and the gate voltage at $2f_0$= 14 MHz; a lock-in detector measures the vibration amplitude.

The modulation of the spring constant is expressed in normalized units as a pumping factor h. At the amplification working point ("Maximum" in Fig. 2), the gain increases continuously as h approaches 1, its theoretical upper bound (above h=1, the system starts to self-oscillate). At the "squeezing" working point (point "Minimum" in Fig. 2), the gain tends towards ½. These are characteristic features of the parametric amplification scheme.

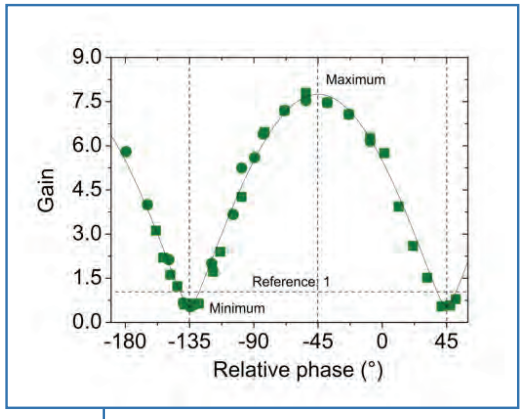

Figure 2: Phase dependence of mechanical gain. One can amplify (point "Maximum"), or squeeze (point "Minimum") the mechanical vibrations depending on the relative phase between the 7 MHz test force and the 14 MHz spring-constant modulation. The line is a theoretical fit, with parametric pumping factor h=0.87.

Of course, the actual gain obtained at the limit h=1 is never infinite, but limited by unavoidable experimental imperfections. With our device, amplification of the driving force with gains up to a 100 has been achieved, see Fig. 3. This is exceptional for an oscillator that is moving about 5 nm, a substantial fraction of its thickness, under these optimal conditions.

We have developed a theoretical model to describe the limiting parameters of this parametric amplification scheme. Our model has been applied to study the fine structure of the friction mechanisms occurring in the metallic coating films deposited on the nano-mechanical device. An unprecedented resolution of 0.5 % in the damping coefficient has been achieved in our measurements.

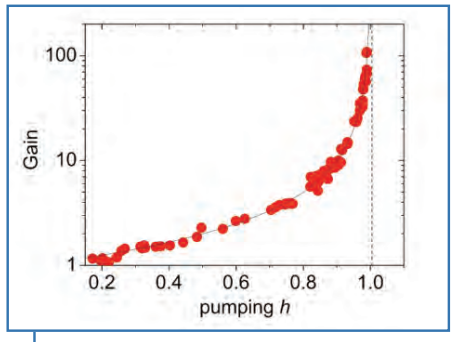

Figure 3 : Mechanical gain measured at the phase setting "Maximum" of Fig. 2 as a function of pumping factor h. The line is a theoretical fit, and h=1 is the limit of the amplifying scheme.

CONTACTS
Eddy COLLIN
eddy.collin@grenoble.cnrs.fr
Olivier BOURGEOIS
olivier.bourgeois@grenoble.cnrs.fr

Ph.D STUDENT
Martial DE FOORT

FURTHER READING

NONLINEAR PARAMETRIC AMPLIFICATION IN A TRI-PORT NANOELECTROMECHANICAL DEVICE
E. Collin, T. Moutonet, J.-S. Heron, O. Bourgeois, Yu. M. Bunkov, H. Godfrin
Phys. Rev. B 84, 054108 (2011).

XPAD detectors: from the laboratory to industrialization

Hybrid pixel detectors will mark the end of the era of CCD cameras in numerous experiments using X-rays. The "XPAD" technology, born of a collaboration involving the Néel Institute, is one example of such a detector. This development has produced three generations of XPAD detectors and has led to the birth in 2010 of imXPAD, a startup company dedicated to production and commercialization of these detectors. Initially, hybrid pixel detectors were designed for particle physics. In the 1990's, experiments done on the new synchrotrons, such as the European Synchrotron Radiation Facility (ESRF) in Grenoble, suffered from the lack of X-Ray detectors with fast enough dynamics to exploit the new potentialities offered by synchrotron X-Ray beams. Since then, Néel Institute staff in charge of the French Collaborative Research Group beamline "D2AM" at the ESRF have worked with people at the Centre de Physique des Particules in Marseille (CPPM) and the SOLEIL synchrotron (Paris) to develop three generations of the "XPAD" hybrid pixel detector technology.

XPADs (X-ray Pixel chips with Adaptive Dynamics) have many advantages over earlier detectors. They are hybrid pixel detectors : silicon sensors are "bump-bonded" directly, pixel by pixel, to an underlying, dedicated electronics chip. They measure the position and the number of incident photons with specific new characteristics compared to the CCD (Charge Coupled Device) detectors used previously. In CCD cameras, X-ray photons are converted to visible light which is accumulated over a given period. In these new detectors, the X-Ray photon counts are processed individually and only the events above a certain energy threshold are counted, reducing spurious noise sources. In addition, with XPADs one can accumulate many more photons without reaching saturation, therefore gaining in dynamic range, and one can record more than 1000 frames per second. Further, the 3rd generation detector "XPAD3" has an electronic shutter which can be triggered by an external signal, allowing nanosecond resolution in time-resolved experiments. The performances achieved by XPADs allow us to envisage new synchrotron experiments that would have been impossible with conventional detectors. Moreover, these detectors will also find their place in laboratory experiments and in medical X-Ray applications.

The initial role of Néel Institute staff in the XPAD project was to start up the collaboration and define the key features of the electronics chips: dynamics, counting rate, energy resolution, pixel size, etc. Subsequently, our main role has been the testing and calibration of XPAD detectors using synchrotron radiation. To illustrate the performance of XPADs, we present (Fig. 2) some X-Ray diffraction results obtained on the D2AM beamline. These concern the structural and compositional properties of Indium Gallium Nitride (InGaN) alloy "core-shell" nanowires, properties important for optimizing the nanowires' emission wavelength. The extended DAFS (Diffraction Anomalous Fine Structure) spectra give information on the In content and the local atomic environment of the resonant atoms (Ga), i.e. they show how the strains resulting from the unequal sizes of Ga and In atoms are accommodated locally.

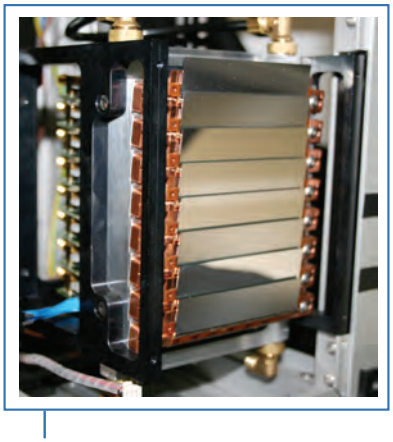

Figure 1 : Inside a prototype Silicon XPAD3 detector : 8 modules are tiled as close as possible to each other to offer a 7x12 cm² detection surface with almost 540000 pixels of size 0.13x0.13 mm².

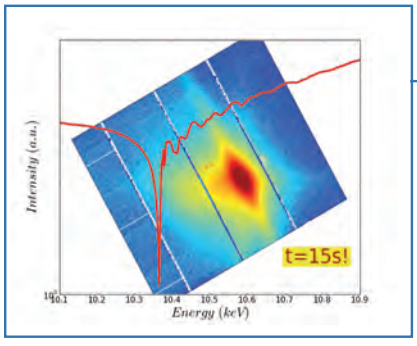

Figure 2: From an X-Ray diffraction study of InGaN core-shell nanowires grown on GaN : The red trace is a Diffraction Anomalous Fine Structure (DAFS) spectrum extracted from reciprocal space maps at several energies from 10.1 keV to 10.9 keV. One such map is put, color-coded, as the background 2D image. Around the intense GaN (101) reflection (red, brown) coming from the substrate, the map shows a surrounding signal (yellow, green) due to the scattering of the InGaN core-shell nanowires. The measurement was performed at the Gallium K-edge without attenuators using a XPAD3 pixel detector on beamline D2AM at the ESRF. The quality of the DAFS spectrum acquired in only 15 seconds is remarkable.

Here, the main interest of the 2D pixel detector XPAD is the high counting dynamics per pixel, which allows us to benefit from the high counting rate for diffracted X-Ray photons when measuring DAFS oscillations. Moreover the detector allows measurement of several DAFS spectra and the fluorescence background simultaneously.

At present, XPAD detectors use well-tested silicon sensors, but detection efficiency is quickly lost for X-Rays from 15-20 keV onwards. In parallel, we have also worked on using more efficient sensors. We have obtained very good results with prototype Cadmium Telluride (CdTe) sensors. These are available only in limited sizes so far and it is intended to continue our collaboration with CPPM-Marseille and SOLEIL to create CdTe detectors with larger surfaces.

CONTACTS

Nathalie BOUDET
nathalie.boudet@grenoble.cnrs.fr
d2am@esrf.fr

Jean-François BERAR
jean-francois.berar@grenoble.cnrs.fr
d2am@esrf.fr

FURTHER READING

XPAD3-S : A FAST HYBRID PIXEL READOUT CHIP FOR X-RAY SYNCHROTRON FACILITIES
P. Pangaud, S. Basolo, N. Boudet, J-F. Bérar et al.
Nucl. Instr. and Meth. A 591, 159 (2008).

PERFORMANCE AND APPLICATIONS OF THE CDTE- AND SI-XPAD3 PHOTON COUNTING 2D DETECTOR
K. Medjoubi, S. Hustache, F. Picca, J.-F. Bérar, N. Boudet et al.
J. Instrumentation 6, C01080 (2011).

The turbulent superfluid cascade

Stirring a honey pot with a spoon is awkward because the fluid viscosity damps the flow very efficiently. By contrast, in a less viscous fluid such as coffee in a cup, a slight movement of a spoon will generate eddies of different sizes. If the fluid is even less viscous, or if the mechanical stirring is more intense, a hierarchy between eddies of different sizes appears: the flow is turbulent. In 1941, the Russian mathematician Andrei Kolmogorov described this hierarchy of eddies with the image of an energy cascade : mechanical stirring feeds the largest eddies, which transfer their energy to smaller eddies and so on until the viscosity effectively inhibits any further whirling motion and dissipates energy into heat.

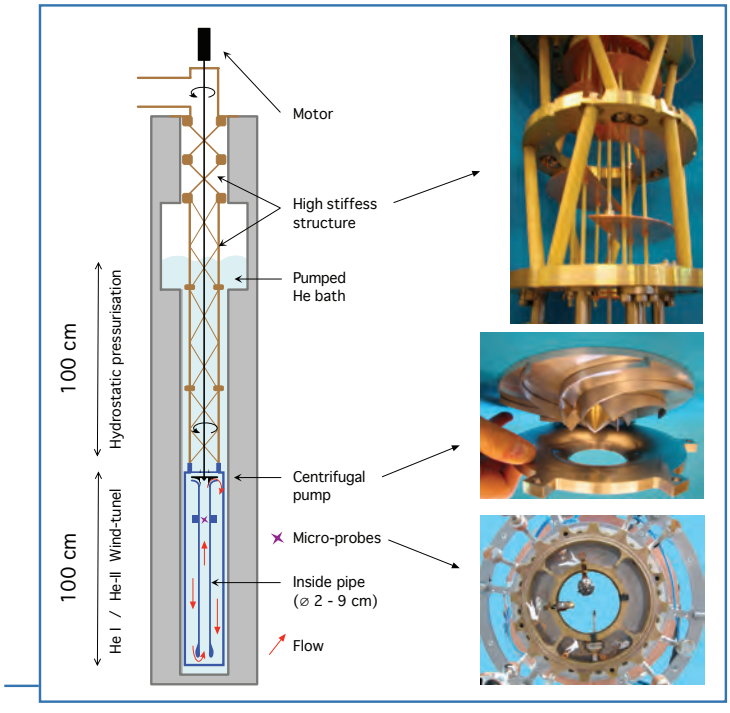

Figure 1: At left: The TOUPIE wind-tunnel. At right: Details of the high-stiffness, low-conductivity mechanical structure (top); Cryogenic propeller specially optimised for liquid helium (middle); Probe holders with miniature Pitot-tube velocity sensors (bottom).

What does this cascade of energy become in a fluid with zero viscosity ? An exotic liquid allows us to address this question experimentally : superfluid helium. Below 2.17 K, liquid helium enters a quantum phase, the "He-II" state. It then acquires the remarkable capability of flowing without experiencing any viscosity. Exploring the turbulent cascade of a superfluid, however, raises two experimental challenges: creating a suitable cryogenic flow and probing the velocity fluctuations in the superfluid.

To answer these questions, the Institut Néel has developed a cryogenic "wind tunnel". We have named this apparatus "TOUPIE" (our acronym for "TOUrne Par l'Intérieur et l'Extérieur", refering to the rotational degrees of freedom in the design of the experiment, and also the French word for a spinning top). It produces a closed, permanent flow of liquid helium along a record path of 2 metres (see Fig. 1) at temperatures from 4 K down to 1.5 K. It can operate with superfluid helium (He-II), and also with "viscous" liquid helium (the "He-I" state, above 2.17 K), thereby allowing direct comparison between the two cascades. The second challenge was to improve significantly the spatial resolution of the best probes for measuring velocity in a superfluid. Among the innovative sensors devised and developed, the one shown in Fig. 2 is a micro-machined silicon cantilever, coupled to an ultra-sensitive superconducting resonator diverted from its original astrophysics destination: the detection of cosmic particles.

The combination of this unique cryogenic wind tunnel with the smallest superfluid probes allowed us to compare the turbulent cascades of a classical fluid with those of a superfluid, with an unprecedented resolution. In particular, we found the first direct evidence that superfluid eddies can cascade from large to small scales in a fashion similar to that of classical eddies. This evidence came from the Kármán-Howarth "4/5 law", the only exact relation in turbulence (named after a factor 4/5 in the equation that relates the amount of energy carried by the turbulent cascade and a dissymmetric statistics of the velocity gradients). Comparing our data with the Kármán-Howarth law, we found that this law remains valid in a superfluid.

The next challenge is to understand how, in the superfluid, a non-viscous dissipation process replaces the effects of viscosity, especially in the limit of relatively low temperatures (~ 1 K). A second version of the TOUPIE wind-tunnel is in preparation to reach this lower temperature range.

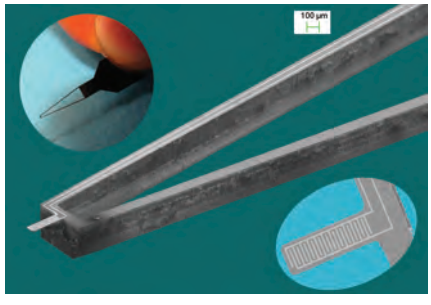

Figure 2: Micro-machined velocity probe based on the deflection of a 1 micron thick, 100 micron wide, silicon cantilever by the moving fluid. Main image shows the V-shaped probe-holder with the cantilever at its tip. The upper insert shows a general top-view onto the probe holder. The bottom insert is a zoomed top-view of the cantilever itself, carrying a circuit which is part of a superconducting resonator whose frequency varies with the cantilever's deflection. Device fabricated at Grenoble's "Plateforme Technologique Amont".

CONTACT
Philppe-E. ROCHE
per@grenoble.cnrs.fr

Ph.D STUDENT
Julien SALORT

FURTHER READING

ENERGY CASCADE AND THE FOUR-FIFTHS LAW IN SUPERFLUID TURBULENCE
J. Salort, B. Chabaud, E. Leveque, and P.-E Roche, Europhys. Lett. 97, 34006 (2012).

Improved diamond devices with low active defect concentrations

Diamond is a "wide bandgap" semiconductor: E_G=5.4 eV, five times larger than that of silicon. It is considered as the ultimate material for fast, high voltage and high power electronics. Metal/diamond Schottky diodes and Metal/Insulator/Semiconductor (MOS) structures can now be fabricated in epitaxial diamond films grown on bulk diamond crystals. However, the device performance can be limited by defects or unwanted impurities located inside the diamond active layer. Using extremely sensitive electrical measurement techniques, we have now identified the principle defects restricting the flow of hole carriers in p-type diamond films, and we have investigated new growth techniques for eliminating them.

This work concerns the electrical properties of epitaxial diamond films grown at the Néel Institute on commercially available diamond substrates. The films are doped with the acceptor impurity boron to obtain p-type conductivity. Control of lattice defects and undesired impurities is essential, as these can trap carriers flowing in the valence or the conduction band. The defects are present in very low concentration, below the detection thresholds of most analysis and characterisation techniques. But they can be detected by their change in electronic charge or the transient current flowing in the bands when they release the trapped carriers (Deep Level Transient Spectroscopy measurements).

The measurement of the populations in the different charge states is done using a Schottky diode (Fig. 1). Through a voltage bias pulse applied to the Schottky electrode, the defects can be charged with holes to a non-equilibrium state. Capacitance transients or current transients are then measured when holes, initially trapped in a deep level pertaining to some defect, are emitted into the valence band. These transients are thermally activated because statistical thermodynamics apply in such a way that the emission rate increases with temperature.

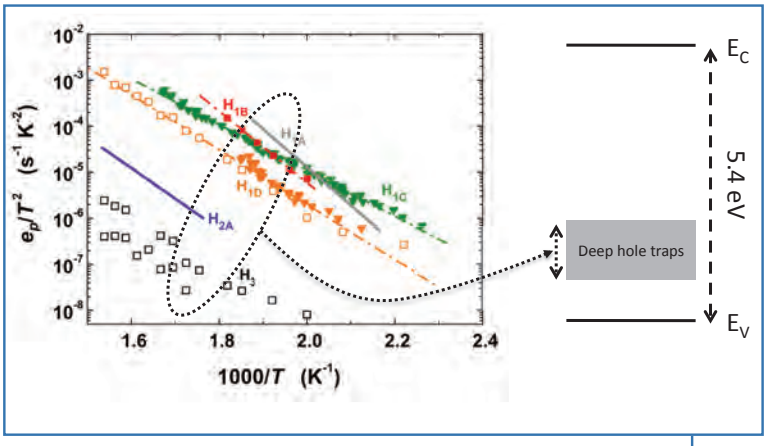

Figure 2: At left: Arrhenius diagram for deep hole traps in boron-doped diamond layers. The hole emission rate e_p divided by the square of the temperature is plotted against 1000/T. At right: energy range of the deep hole traps detected in the diamond band gap.

The emission rates are monitored as a function of temperature, via Fourier transforms of the transients (Fig. 2). This enables us to derive the ionization energy of the hole trapping defects, which is the main property for defect identification, as well as their concentration.

Many defects with hole ionization energies in the range 0.5-1.6 eV are detected (Fig.2). Theoretical calculations show that most of them can be attributed to complex centres comprising one or several atoms of boron and hydrogen, in some cases associated with a lattice vacancy (a missing carbon atom).

We have confirmed the role of hydrogen by preparing diamond layers with a small additional percentage of oxygen in the gas phase. This is known to dramatically decrease the H density on the surface and H incorporation in the bulk. These layers no longer show any hydrogen related deep levels. Consequently, this new recipe for diamond epilayer growth guarantees a defect-free material, at least for the deep levels due to hydrogen associated with boron atoms and/or a carbon vacancy.

Figure 1: Schottky diode device fabricated on a diamond epilayer. These devices are used for determining the concentrations and ionisation energies of carrier-trapping defects

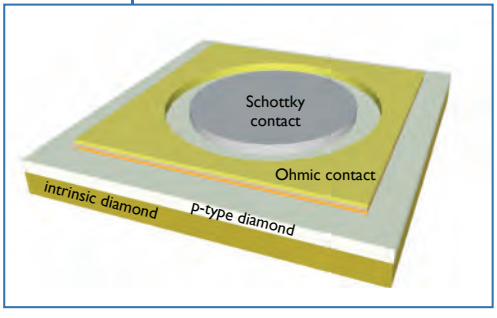

CONTACTS

PIERRE MURET
pierre.muret@grenoble.cnrs.fr

Julien PERNOT
julien.pernot@grenoble.cnrs.fr

Ph.D STUDENT
Pierre-Nicolas VOLPE

FURTHER READING

DEEP HOLE TRAPS IN BORON-DOPED DIAMOND
P. Muret, J. Pernot, A. Kumar, L. Magaud, C. Mer-Calfati and P. Bergonzo
Phys. Rev. B 81 (2010) 235205.

HOLE TRAPS PROFILE AND PHYSICAL PROPERTIES OF DEEP LEVELS IN VARIOUS HOMOEPITAXIAL DIAMOND FILMS
P. Muret, P.-N. Volpe, J. Pernot, F. Omnès
Diamond & Related Materials 20 (2011) 722.

Superconducting Artificial Atom

Quantum mechanics was developed initially to describe properties of electrons in atoms which could not be explained by the classical laws of physics. During the last decade, nanometre scale superconducting electrical circuits incorporating tunnel junctions for the superconducting electrons (Josephson junctions) have revealed puzzling properties at very low temperature that deviate from the classical laws of macroscopic electricity. Quantum mechanics is needed to describe the current and voltage behaviour of these circuits. Contrary to the hydrogen atom in which the wavefunction describes a single electron, in the superconducting circuit one has a macroscopic quantum state of all the superconducting electrons. However, because there are certain similarities to atoms, such as the quantization of energy levels, superposition of quantum states, and the interaction with an electromagnetic field, we call these circuits "artificial atoms".

The interesting feature of such an "artificial atom" is that its characteristics are not rigid as in a real atom but controllable by the experimentalist. Indeed, they are not defined by a fixed number of electrons and protons as in a real atom but by properties of the circuit (its capacitance, inductance, tunnel barrier). These are adjustable during the nano-fabrication process. In addition, the artificial atom's quantum states can be readily manipulated by external magnetic flux or microwaves.

Currently, most of the superconducting artificial atoms studied are described by a single, anharmonic quantum oscillator. For instance, this is realized by circuits containing a single Josephson tunnel junction. The equivalent circuit is an "LC" electrical resonator, made up of a capacitance C and a non-linear inductance L associated with the Josephson junction. The total energy of the superconducting electrons is quantized. (When only the two first levels are considered, the artificial atom can act as a "quantum bit").

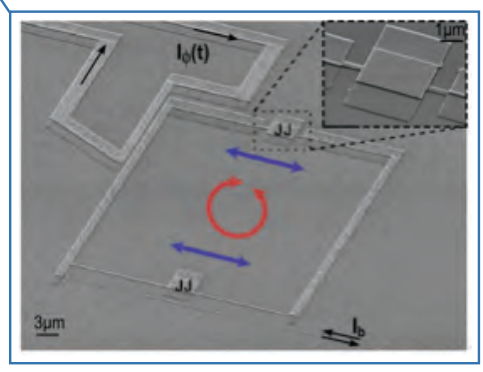

Figure 1: Scanning Electron Microscope image of a superconducting "artificial atom". It consists of a highly inductive loop of aluminium wire with two Josephson tunnel junctions (JJ) made by two overlapped Al layers separated by a thin aluminium oxide layer (see zoom top right). The circuit is superconducting below 1.5K and the quantum experiments are realized at 40mK. The modes "s" and "a" (schematized by blue and red arrows, respectively) are excited by applying external microwave currents $I_\Phi(t)$ or $I_b(t)$.

In our own recent work, we have studied a circuit with *two* tunnel junctions (see Fig. 1), producing a new type of artificial atom described by two strongly coupled anharmonic oscillators. This leads to two modes labelled "s" (symmetric) and "a" (anti-symmetric) because the current oscillations at each junction can be either in-phase or in phase-opposition, respectively.

We apply a variable frequency microwave flux through the circuit to induce excitations of the two modes and thus determine their quantized energy level spectrum. Furthermore, we can tune the energies of the quantized states by applying an external magnetic field. Fig. 2(a) gives the field-dependence of the transitions from the ground state |0a, 0s> to the first 4 excited states. In particular, the Figure shows an anti-crossing of two levels (dotted green square) which demonstrates a non-linear coupling between the two modes "s" and "a".

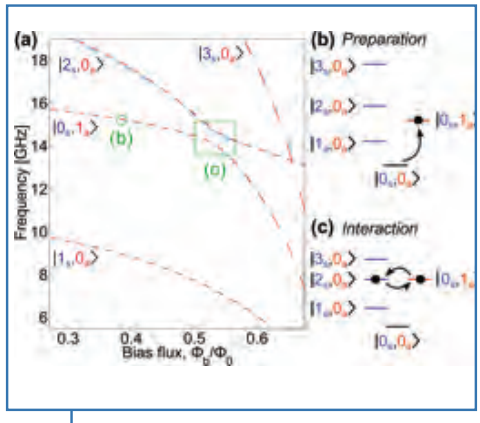

Figure 2: (a) Energy spectrum of the artificial atom of Fig. 1 versus applied magnetic flux (in units of the flux quantum Φ_0), from microwave spectroscopy (blue curves) and a theoretical fit (red curves). (b), (c); Quantized energy spectrum of the two anharmonic oscillators at (b) $\Phi=0.37\Phi_0$ and at (c) $\Phi=0.54\Phi_0$. In (b) the system is prepared in the state |0s, 1a> and in (c), following an ultrafast flux jump, coherent oscillations occur between states |0s, 1a> and |2s, 0a>, producing up and down frequency conversion.

In another experiment, the non-linear coupling between the two modes leads to coherent up and down frequency conversion, see Figs 2(b), 2(c). At $\Phi=0.54\ \Phi_0$, the state |0s, 1a> (one excitation at frequency 14.4 GHz in the anti-symmetric mode) evolves to the state |2s, 0a> (two excitations at about 7.2 GHz in the symmetric mode). The coherence of this process is demonstrated by the observation of free oscillations between the states |0s, 1a> and |2s, 0a> of the two modes.

The non-linear coupling terms observed in our artificial atom are orders of magnitude larger than those studied in atomic physics and non-linear optics, leading to new properties and also to a novel method for fast quantum "non-demolition" measurements.

CONTACTS
Olivier BUISSON
olivier.buisson@grenoble.cnrs.fr
Wiebke GUICHARD
wiebke.guichard@grenoble.cnrs.fr

Ph.D STUDENT
Florent LECOCQ

FURTHER READING

NON-LINEAR COUPLING BETWEEN THE TWO OSCILLATION MODES OF A DC-SQUID
F. Lecocq, J. Claudon, O. Buisson and P. Milman
Phys. Rev. Lett. 107, 197002 (2011).

COHERENT FREQUENCY CONVERSION IN A SUPERCONDUCTING ARTIFICIAL ATOM WITH TWO INTERNAL DEGREES OF FREEDOM
F. Lecocq, I. M. Pop, I. Matei, E. Dumur, A. Feofanov, C. Naud, W. Guichard, O. Buisson
Phys. Rev. Lett. 108, 107001 (2012).

Flexural-hinge micro-positioning device for synchrotron experiments

Flexural hinges are used more and more in microsystem technology. Recently, the Néel Institute's technical services (SERAS) were requested to manufacture and to simulate the behaviour of a compact positioning device to be dedicated to an X-Ray beamline at the European Synchrotron Research Facility (ESRF), Grenoble. The purpose of this assembly is to position a sample in the X-Ray beam with an isotropic precision of a few microns. It is mounted on a robotic manipulator, which is part of a bench for transfer of crystal samples to the goniometric head of an X-Ray diffractometer. The main technical challenge of the system lies in a hardened steel part of complex shape.

For precision microsystems, mechanical functions such as guidance and positioning need to be reconsidered in order to operate without friction. The flexural hinge ("*charnière*") or "flexor" satisfies this requirement. But, although this technology has been known for many years, detailed information about its implementation is relatively scarce. Among the available solutions, the "circular notch" shown in the insert of Fig. 1 offers many advantages. The mechanical part is bent elastically around its thinnest section - the hinge. There is no friction (so no lubricant needed), and no backlash ("*jeu*"). The monolithic hinge requires no assembly, the device can be very compact and very precise.

The multiple hinge positioning mechanism described here (Figs 1 and 2) was requested for the French beamline for Investigation of Proteins (FIP- BM30A) at the ESRF. Its purpose is to give the final position of the sample in the X-Ray beam. The fixed part of the hinge (tinted green in Figs 1,2) is mounted onto a robotic arm ("GRob") which gives the coarse position. Two, linear, stepper-motion, piezo-actuators drive displacement of the moving part of the hinge (pink in Figs 1,2) over a 5 mm diameter area with micron precision. The moving part is equipped with a pneumatic device which attaches the sample holder. The plane of movement (horizontal in the photos) is vertical in the experiment, so a very strong part is needed to support the hanging weight of the sample holder.

Based on the ESRF's design, the goals of our participation were to check the technical feasibility for machining the main flexor component, to manufacture the first prototypes and to carry out numerical simulation to optimize the design. The design required a hardened steel part of complex, articulated shape with 16 hinges (Fig. 1). This component was to be machined with an Electrical Discharge Machine (EDM) process, leaving a 100 micron thickness of steel for each of the hinges. Extensive tests and three prototypes were necessary to work out the operational procedure and to achieve the geometrical specifications.

The other main problem is the high mechanical properties of the 100Cr6 alloy used (yield strength 2200 MPa after heat treatment), incompatible with the hardness of standard tooling, especially for machining the tapped holes. The following manufacturing process in four phases enabled us to obtain a part satisfying all the requirements: (1) outline contouring, drilling and tapping of holes; (2) hardening heat treatment to achieve the required tensile properties (yield strength, hardness); (3) final surface grinding to reach the tolerance on the part's surfaces and thickness; (4) outline and section machining of the 16 hinges with the EDM process. In phase (4), approximately 30 machining programs were necessary to realize the final flexor part (Figs 1 and 2). It represents 70 hours of cutting.

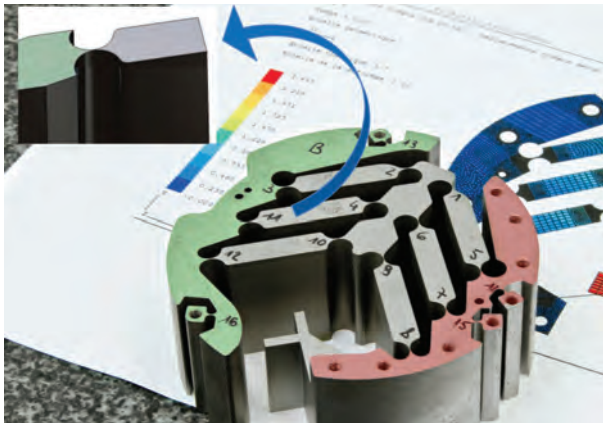

Figure 1: First prototype of flexor part at end of phase 4, before assembly (fixed part tinted green, moving part tinted pink). Insert at top left shows detail of a circular notch. In the background a plot of the finite elements model of the displacement field.

In tests of the first prototype, metal fatigue occured after a relatively small number of cycles. Finite element calculations were performed to understand the strain mechanisms, to determine the stress areas and to give recommendations for a new design. Due to local yielding these calculations were necessarily non-linear. The recommendations were to increase the overall thickness (height) of the part from 15mm to 30mm, and to change the design and position of the tapped holes and the mechanical stop clearance.

This work involved J-L. Ferrer and M. Terrien (design) at the ESRF and P. Jacquet (machining) and V. Roger (calculations) at Néel Institute. The machining project ran for 8 months and is completed. Work is now focused on control and command aspects before the device becomes fully operational.

Figure 2: The final prototype of the Flexor during assembly, shown equipped with one piezoelectic actuator. At right, the metal part at the end of phase 2 (heat treatment).

CONTACTS

Philippe JACQUET
philippe.jacquet@grenoble.cnrs.fr

Emmanuel ROY
emmanuel.roy@grenoble.cnrs.fr

When electrons perform in quartets

Superconductivity is due to the condensation of a fraction of the electrons into Cooper pairs. A Josephson junction is a short bridge between two superconductors which allows a coherent transfer of Cooper pairs. Connecting three superconductors in a narrow region realizes a "bijunction". In such bijunctions, part of the superconducting currents must flow as correlated Cooper pairs, which are referred to as "electron quartets". New quantum correlations could be revealed in a bijunction, which is characterized by two phase variables coupled together, instead of one.

A superconductor is characterized by a mutual attraction between electrons at the Fermi surface, due to lattice phonons. This results in the formation of the famous Cooper pairs, which condense into a phase-coherent collective state at low temperature. In the classical superconductors used in nanofabrication (such as a Aluminium or Niobium), this collective state is well described by the Bardeen-Cooper-Schrieffer (BCS) theory of superconductivity.

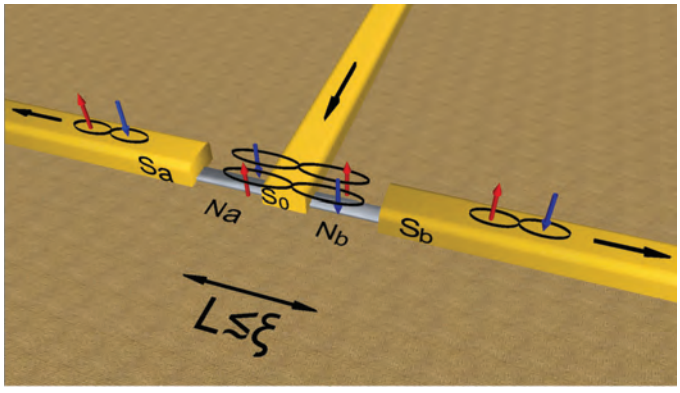

Schematics of a bijunction consisting of three superconducting leads (yellow), separated by two, narrow non-superconducting regions N_a, N_b (grey) at the size scale of the Cooper pair ξ (at most a few hundred nm). The "quartet" component of the current flows from the central lead S_0 via the splitting of two singlet Cooper pairs, each into a spin up and a spin down electron. The spin of the electrons is indicated by blue and red arrows. Subsequently the quartet recombines into one Cooper pair exiting in lead S_a and another in S_b. A phase-coherent quartet current can flow even in presence of voltage biases, if $V_a = -V_b$.

Josephson discovered 50 years ago that two BCS superconductors separated by a thin oxide layer can exchange Cooper pairs. This maintains phase coherence and leads to a dissipationless dc supercurrent tunneling through the junction. This current exists only at zero voltage across the junction. A Josephson junction is characterized by the two Josephson equations, one for the relation between the current and the phase-difference across the junction at zero voltage and the other for the linear time dependence of the phase difference at constant voltage.

We have proposed that in a "bijunction" (see the Figure), where two side current leads S_a, S_b are fed by a central lead S_0 at a scale $L \lesssim \xi$ the Cooper pair size, a new microsocopic mechanism leads to the formation of electronic "quartets". A first Cooper pair entering from lead S_0 splits virtually into two electrons, one exiting in lead S_a and one in S_b. A second Cooper pair immediately splits in the same way, and the so-formed "quartet" of electrons eventually redistributes into one Cooper pair in S_a and one Cooper pair in S_b (see Figure), with a remarkable sign change of the quartet current compared to an ordinary junction. The quartets are transient states and can be understood as a four-particle resonance in the bijunction.

Strikingly, our calculations show that phase-coherent dc resonances can occur even in the presence of non-zero applied voltages V_a, V_b, with $V_0 = 0$. This is due to the quartet process in which two Cooper pairs from S_0 are transmitted simultaneously as one pair in S_a and one pair in S_b. The energy of the final state is $2e(V_a + V_b)$ and the energy of the initial state is 0. Then the energy is conserved if Va = -Vb. By the Josephson equations, this implies that a dc current of quartets appears just at the resonance condition $V_a = -V_b$. This current is phase-coherent, just like the ordinary zero-voltage DC Josephson current. Higher order resonances are also expected when $nV_a + mV_b = 0$, where n, m are integers. They are currently being tested experimentally.

In the future, nanoscale interference devices for the supercurrent inspired from the Superconducting Quantum Interference Devices (SQUIDs) will be an appropriate tool for probing these quartets because they have very specific signatures in the Josephson relationship linking the currents to the phase differences.

Josephson bijunctions are new objects, and the correlations between four electrons in a quartet open perspectives in the study of four-electron entanglement. They should also lead to nonlinear parametric amplification at microwave frequencies, if microwave lines are coupled to the bijunction.

CONTACTS

Régis MELIN
regis.melin@grenoble.cnrs.fr

Denis FEINBERG
denis.feinberg@grenoble.cnrs.fr

FURTHER READING

PRODUCTION OF NONLOCAL QUARTETS AND PHASE-SENSITIVE ENTANGLEMENT IN A SUPERCONDUCTING BEAM SPLITTER
A. Freyn, B. Douçot, D. Feinberg and R. Mélin
Phys. Rev. Lett. 106, 257005 (2011).

Frequency-to-current conversion with coherent Josephson crystals

This project will explore quantum mechanical coherence in Josephson crystals and apply it for frequency-to-current conversion. A Josephson "crystal" can be realized by repeating a single Josephson junction or SQUID in space to form a one-dimensional ladder structure. This crystal can show a macroscopic coherent behaviour due to the coherent superposition of the quantum "phase-slips" (2π phase differences) occurring on each single junction. The coherent superposition gives rise to a novel, global non-linearity which turns the Josephson crystal into an effective "single junction" described by the dynamics of the global charge.

The enormous progress in the control of the microwave environment in superconducting quantum circuit experiments over the last ten years now makes it possible to study coherence in large multi-junction circuits experimentally. In particular this project aims, by novel experiments on Josephson junction chains, to understand the crucial questions of external charge dynamics and dissipation that originate from the many-body effects present in these chains. Scaling up the number of Josephson junctions in a circuit automatically implies the presence of low-frequency plasma modes, which lead to internal dissipation in the system and make these experiments very challenging.

By using Josephson junction chains with a disordered or fractal pattern it should be possible to localize plasmon wave-functions that do not couple to the quantum states of the Josephson crystal and simultaneously keep the coherence intact. In addition, a first systematic study will be done of the external charge dynamics occurring in Josephson junction chains, in particular noise correlations.

A final aim of the project is to use the coherent superposition of quantum phase slips in a Josephson crystal to realize a frequency-to-current converter. If successful, this project will lead to a definition of the electrical current with an unprecedented precision.

CONTACT
Wiebke GUICHARD
wiebke.guichard@grenoble.cnrs.fr

ERC STARTING GRANT 2012

Hybrid quantum nano-optomechanics

It has recently become possible to cool macroscopic mechanical oscillators down to their quantum ground state of motion. Various kinds of mechanical oscillators, ranging in mass from picograms to micrograms have now been prepared at ultralow mean phonon occupancy by combining traditional cryogenic and active cooling techniques. It is now time to envision even more challenging experiments aiming at "engineering" the quantum mechanical state of the oscillator. This can be achieved by coupling the ultracold oscillator to a second system whose quantum state can be independently controlled and transferred onto the mechanical oscillator. The combination of these two components defines a "hybrid" mechanical system.

This project aims at exploring the emerging field of hybrid quantum nano-optomechanics in a setting where both components of the system can be monitored and controlled simultaneously. The goal is to investigate the hybrid coupling between a nanomechanical oscillator and a Nitrogen Vacancy defect in diamond. The electronic spin state of the defect represents a unique quantum system, of exceptional quality, which can be readout and manipulated by optical means. The nanoresonators will be probed by exploiting the ultrasensitive optical techniques developed in the context of cavity optomechanics. When combined with the intrinsic, extremely high force sensitivity innate to nanomechanical oscillators, this approach promises to give unprecedented sensitivity for exploring the subtle signatures of the hybrid interaction. The goal of the project is to enter the quantum regime of hybrid nano-optomechanics and investigate unexplored phenomena, at the interface between the classical and quantum worlds.

CONTACT
Olivier ARCIZET
olivier.arcizet@grenoble.cnrs.fr

ERC STARTING GRANT 2012

INTERNAL WORKSHOP

30-31 MAY 2012

In May this year, researchers, technical and administrative staff, PhD students and postdocs of the laboratory contributed to the "Journées NEEL", an internal workshop of the NEEL Institute, five years after its creation. About 300 members of the laboratory attended this two-day event, mainly devoted to presentations and discussions concerning the organization and scientific strategy of our Institute. Thanks to the efforts of the many colleagues who prepared and led the multiple workshops and sessions, many constructive ideas were outlined that should bear fruit in the future. We benefited considerably from several external contributions, in particular as concerns three thematic workshops on energy, bio-sciences and materials. In addition, our discussions were stimulated by a lecture by Nayla Farouki on the philosophy of innovation and talks by Sylvestre Huet and Jean Lilensten on science mediation.

Propagative and Internal Coherence in Semiconductor Nanostructures

This project concerns the field of coherent, nonlinear, ultrafast, light-matter interaction on a quantum level in solids. It will explore experimentally the limits of: i) the internal coherence of an individual light emitter; ii) the radiative coupling between a pair of emitters. The individual emitters to be employed are excitons in semiconductors: either loosely bound to impurities or strongly confined in quantum dots.

CONTACT
Jacek KASPRZAK
jacek.kasprzak@grenoble.cnrs.fr

ERC STARTING GRANT 2012

First, by embedding the emitters in photonic nanowires produced in Grenoble, collection of the coherent optical response of individual emmiters will be amplified by nearly four orders of magnitude. This will provide unprecedented access to the emitters' coherent interaction with phonons and their dephasing. The second objective is to demonstrate an efficient, controllable and non-local, coherent coupling mechanism between distant light emitters, which is a prerequisite for the construction of quantum logic gates and networks. Here, the aim is to demonstrate a radiative coupling — effectively a "wiring-up" of two emitters via a propagating electromagnetic field — using resonant quantum emitters embedded into in-plane one-dimensional waveguides, which permit virtually unattenuated propagation of coherence. The internal and propagative coherence of individual emitters and radiatively coupled pairs will be explored using methods of coherent nonlinear spectroscopy beyond the current state of the art. Specifically, in order to demonstrate radiative coupling, a heterodyne spectral interferometry technique with spatial resolution will be developed.

For the remaining and the most challenging part of the project, this advanced spectroscopy technique will be combined with ultrafast pulse-shaping in order to perform long-range coherent manipulation within a pair of exciton-biexciton systems in two strongly-confining quantum dots. Achievement of this goal should enable performing logical operations between distant emitters, paving the way towards optical quantum information processing based on semiconductor technology.

Quantum Coherence and Manipulation of a Single Flying Electron Spin

In quantum nanoelectronics, a major goal is to use quantum mechanics in order to build efficient nanoprocessors. This requires the ability to control electronic phenomena in a nanostructure at the single electron level. In this context, the electron's spin has been identified as an appropriate degree of freedom for efficient storage and manipulation of quantum information. The defined building block of this quantum computer strategy is called a spin qubit. Towards such goals, intense experimental effort has been invested in AlGaAs heterostructures where quantum dots containing just one electron can be realized.

CONTACT
Tristan MEUNIER
tristan.meunier@grenoble.cnrs.fr

ERC STARTING GRANT 2012

In such a system, an all-electrical quantum manipulation of the spin of a single electron is possible. The implementation of the system as a quantum nanoprocessor resembles the classical circuit boards contained in a classical computer. All the basic operations of a quantum nanoprocessor have been demonstrated in spin qubits and they constitute a very promising platform to study spin dynamics at the single electron level. To scale up the spin qubit system, one has to make two distant qubits interact by exchanging a quantum particle between them. This has been demonstrated recently at the Néel Institute: a single electron has been transferred efficiently between two distant quantum dots on a timescale faster than the spin decoherence time. The aim of the European grant project is to give a new dimension to the spin qubit system by investigating quantum coherence and the manipulation of such a single "flying" electron spin. Displacing a single electron spin coherently not only represents a viable solution towards achieving entanglement between distant qubits but also opens new ways of manipulating electron spins coherently via spin-orbit interaction. The strategy pursued consists in combining single electron transport with the known techniques for measurement and coherent control of a single electron spin in a quantum dot. The new knowledge expected from these experiments is likely to have a broad impact extending from quantum spintronics to other areas of nanoelectronics.

Fluorescent organic nanocrystals embedded in silicate nanoparticles as tracers for in-vivo imaging.

In tumor biology, imaging of new blood vessel growth (angiogenesis) associated with a tumor during its development, and of changes of the tumor's vascular structure after therapy, is important in the evaluation and validation of new treatment protocols. Modifications in the vascular parameters, such as density, blood volume and perfusion, should be followed over time on the same animal tumor model (mouse). Two-photon fluorescence microscopy is the only technique that allows in vivo imaging of these vascular changes at the microscopic scale and deep in the tissue.

In two-photon fluorescence, a molecule is excited by the simultaneous absorption of two photons that combine their energy. This nonlinear effect occurs precisely at the focussed crossing point of the two laser beams, allowing 3D scanning imaging. For this fluorescence imaging technique, we have developed brilliant tracer particles combining several properties: high intensity of the two-photon excited fluorescence, biocompatibility, and large size (several tens of nanometers) to avoid their diffusion across the blood vessel walls. For this purpose, we have synthesized core-shell nanoparticles (NPs) made up of fluorescent organic nanocrystals (the cores) embedded in an amorphous organosilicate (the shells).

These core-shell NPs were obtained from sol-gel solutions containing a solvent, a fluorescent organic dye, the silicon alkoxide precursors of the final silicate shells, and a small amount of water for alkoxide hydrolysis. These solutions were sprayed to form microdroplets, and carefully dried in a laminar gas flow to control the formation of silicate crusts at the droplet surfaces. Confined nucleation and growth of organic nanocrystals in the core of the silicate spheres completed this one-step process (see Fig. 1).

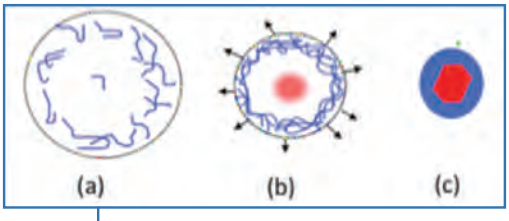

Figure 1 : A droplet drying after sol atomization (a) Initial droplet of homogeneous solution containing the partially hydrolyzed/condensed silicate precursors (blue chains) and the dye dissolved in the organic solvent; (b) Upon drying, a silicate crust is gradually formed at the droplet surface while the confined dye nucleates at the centre; (c) After solvent evaporation, the fluorescent dye is embedded as a single nanocrystal in the core of the organosilicate nanoparticle.

The spray-drying reactor was constructed in our laboratory. The initial sol-gel solutions were drawn into a pneumatic atomizer. The as-produced aerosols, consisting of 1-2 µm droplets, were carried through a laminar air flow, dried gradually at about 150° C in a stainless-steel tube, and collected by electrostatic attraction on exit.

The organic compounds selected for the NP cores were developed by the Chemistry for Optics group of the Ecole Normale Supérieure in Lyon. In the crystalline state they exhibit high 2-photon absorption and high fluorescence emissions in the red and near infrared range, the "biological window" where tissues are transparent. In optimized conditions, the majority (70%) of our core-shell NPs have diameters ranging between 20 nm and 100 nm (see Fig. 2a). The organic cores of the NPs have diameters of order several tenths of nanometers and comprise 10^5-10^7 molecules, yielding fluorescence several orders of magnitude brighter than that of a single molecule. These very brilliant NPs exhibit in general a good photostability, due to their crystallization. Analyzing the crystalline quality of the organic core using Transmission Electron Microscopy in diffraction mode, we obtained well-defined diffraction spots constituting typical patterns for organic single crystals, see the insert in Fig. 2.

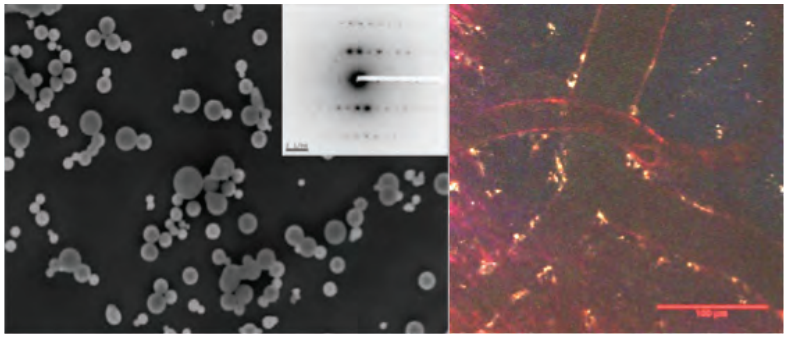

Figure 2 : (a) Scanning Electron Microscope image of nanoparticles prepared from a sprayed sol-gel solution containing CMONS organic dye. Insert in (a): typical electron diffraction pattern showing that the organic cores are single crystals of CMONS. (b) First in vivo, two-photon fluorescence angiography of the microvasculature of the brain of a mouse.

The composition of the silicate shells, which are fully biocompatible and transparent in the visible and near IR, was optimized in a collaboration with the C. Gerhardt Institute, Montpellier University. They allow adjusting the hydrophilicity of the NPs and their subsequent "functionalization" by grafting ligands (peptides) on the NP's surfaces.

Using these new types of nanoparticles, we have done a first in vivo, 2-photon, fluorescence angiography (imaging of blood vessels), at the intravital microscopy platform of the Grenoble Institute of Neurosciences. These first images are very promising as we can clearly see the bright tracers lying on the walls of micro-vessels due to electrostatic attractions (Fig. 2b). This attraction is in fact a typical problem and will be overcome by future developments of the nanoparticle functionalization, aimed in particular at in vivo targeting of the tumor vascular endothelial cells.

CONTACTS

Fabien DUBOIS
fabien.dubois@grenoble.cnrs.fr

Alain IBANEZ
alain.ibanez@grenoble.cnrs.fr

Ph.D STUDENT
Cécile Philippot

FURTHER READING

NANOCRISTAUX FLUORESCENTS ENROBES D'UNE COQUILLE INORGANIQUE
C. Philippot, N. Marcellin, E. Djurado, and A. Ibanez, Patent PCT/FR2009/000294.

NEW CORE-SHELL HYBRID NANOPARTICLES FOR BIOPHOTONICS: FLUORESCENT ORGANIC NANOCRYSTALS CONFINED IN ORGANOSILICATE SPHERES
C. Philippot, F. Dubois, M. Maurin, B. Boury, A. Prat, A. Ibanez
J. Mat. Chem., 22, 11370 (2012).

A new crystal for nonlinear optical generation in the mid-infrared

We have measured the phase matching directions for second harmonic generation and difference-frequency generation in the nonlinear crystal $CdSiP_2$, at infrared wavelengths up to 9.5 µm. By a simultaneous fit to all the angular data, the wavelength dependence of the ordinary and extraordinary principal refractive indices were refined over the entire transparency range of the crystal. This work shows the capability of $CdSiP_2$ for broadband generation of mid-infrared light.

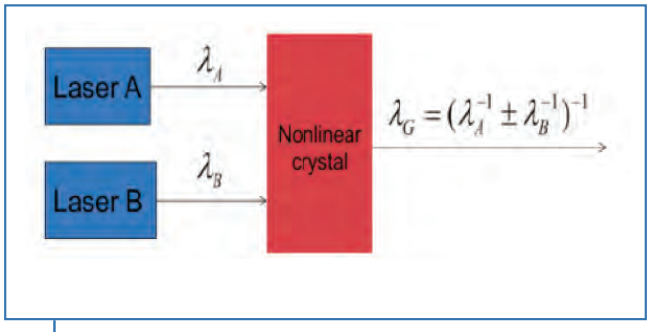

Figure 1 Scheme of sum-frequency generation and difference-frequency generation. λ_A and λ_B are the wavelengths of the incident beams; λ_G is the wavelength of the output wave generated by sum- or difference-frequency interactions

Generating light in the mid-infrared range beyond 5 µm remains an open problem due to the lack of suitable laser sources. Targeted fields of application are medicine, atmospheric telecommunication and spectroscopy. Crystals with strongly nonlinear optical properties appear attractive here because they can convert the wavelength of an incident laser beam into shorter or longer wavelengths via the processes of sum-frequency or difference-frequency generation respectively.

In this context CdSiP2 was recently identified as a promising crystal enabling efficient nonlinear generation near 6.2 µm when pumped by a Nd:YAG laser at 1.064 µm. $CdSiP_2$ is a semiconductor having the tetragonal symmetry, "chalcopyrite" crystal structure. Transparent between 0.56 µm and 10 µm, it exhibits one of the highest second order optical nonlinearities amongst infrared materials. We have performed the first complete measurements of the "phase-matching directions" in the crystal lattice of $CdSiP_2$, as a function of wavelength.

We did this for the two cases of second harmonic generation (SHG), which corresponds to a sum-frequency generation process where the wavelengths of the two incident beams are equal, and difference-frequency generation (DFG). These processes are shown in Fig. 1. The processes have maximum efficiency for propagation along crystal lattice directions where the incoming and outgoing waves have certain, precise, phase relations. The phase-matching condition is related to the dependence of the refractive index on propagation direction and frequency.

The phase-matching angles of $CdSiP_2$ were determined by using a highly accurate sphere cut from a single crystal at Néel Institute. This unique technique has the great advantage of allowing a laser beam to propagate undeviated in any crystal direction. Thus only one sample of the crystal is needed to do a complete and accurate angular variation study. The $CdSiP_2$ sphere was attached to a goniometric head as shown in figure 2. Its tetragonal axis was oriented horizontally with precision better than 0.05° in an automatic X-ray diffractometer before transfer of the goniometric head and sample to the optical bench.

With the sphere at the centre of an Euler circle, it could be rotated about its centre, the direction of the incident laser beams being kept fixed. A focusing lens located at the entrance side of the sphere ensures quasi-parallel propagation of the light beams inside the sample. The wavelength of the incident beams ranged between 0.4 µm and 10 µm. The phase-matching directions and associated conversion efficiencies were recorded for two kinds of processes: second harmonic generation by using as the only input the wavelength tunable beam of a parametric oscillator source; and difference frequency generation by mixing this tunable beam with an auxiliary (YAG laser beam) at 1.064 µm.

Rotating the sphere on itself, we identified the lattice directions for SHG or DFG phase-matching as being the directions where the associated frequency conversion efficiencies were maximum. By fitting all the measured phase-matching curves between 3 µm and 8 µm for single harmonic generation and over 6 µm and 9.5 µm for difference frequency generation, we refined the equations for the wavelength dispersion of the ordinary and extraordinary principal refractive indices. We could then calculate the tuning curve for mid-infrared generation in $CdSiP_2$ via a "parametric fluorescence" process with only a Cr2+:ZnSe laser at 2.4 µm as pump. This would generate simultaneously a super-continuum spreading from 3 µm to 8 µm.

Figure 2 The 5-mm-diameter $CdSiP_2$ sphere placed on the top of a high precision angular positioning stage.

CONTACTS

Benoit BOULANGER
benoit.boulanger@grenoble.cnrs.fr

Patricia SEGONDS
patricia.segonds@grenoble.cnrs.fr

Ph.D STUDENT
Vincent KEMLIN

FURTHER READING

PHASE-MATCHING PROPERTIES AND REFINED SELLMEIER EQUATIONS OF THE NEW NONLINEAR INFRARED CRYSTAL $CDSIP_2$
V. Kemlin, P. Brand, B. Boulanger, P. Segonds, P. G. Schunemann, K. T. Zawilski, B. Ménaert, and J. Debray
Optics Letters 36, 1800-1802 (2011).

A single spin magnetically coupled to a nanomechanical oscillator

The intense experimental efforts of several groups worldwide during the last six years have very recently culminated by demonstrating what the scientific community considered unrealistic only 10 years ago: cooling a macroscopic mechanical oscillator down to its quantum ground state of motion. Experiments going beyond ground state cooling and aiming at generating non-classical states of motion require an actual engineering of the quantum mechanical state of the oscillator. This can best be achieved by coupling the ultracold oscillator to a second quantum system through which one can interact with the oscillator.

The combination of these two components defines a "hybrid" mechanical system. The goal of our research is to investigate these novel hybrid quantum systems consisting of a nano-mechanical oscillator and a fluorescent Nitrogen-Vacancy (NV) defect centre in a diamond nanocrystal. In the work presented here, our system is at room temperature, but we plan to do experiments with ultracold resonators in the future. The electronic spin state of the defect represents a unique quantum system for our purpose: it features ultralong coherence times and can be read out and manipulated with optical and microwave fields. The ultimate goal of the project is to enter the quantum regime of a hybrid nano-mechanical system, where the spin and the oscillator dynamics are entangled, and to investigate phenomena at the interface between the classical and quantum worlds.

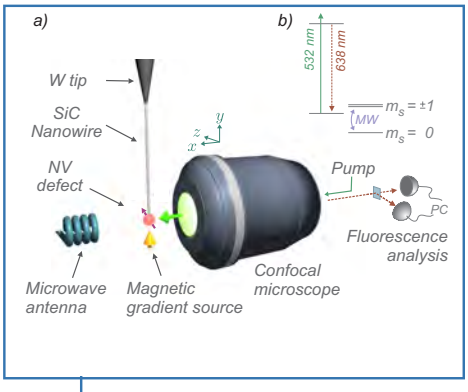

Figure 1 : a) Schematics of the experiment. b) Electronic structure of the NV centre in diamond, which is excited off resonance at 532 nm and fluoresces at 638 nm. The centre's ground state is manipulated with microwave fields (MW).

We have recently taken the first steps in this direction by attaching an NV centre on the vibrating extremity of a SiC nanowire. In order to obtain mechanical control over the nanowire, it was attached at the apex of a tungsten tip, which was positioned on a piezo-electric crystal. The NV fluorescence was collected through a high numerical aperture microscope objective on ultrasensitive avalanche photodiodes (see Fig. 1). The electronic structure of the NV defect exhibits an optical transition in the visible which constitutes a stable single photon source. By recording the emitted photon rate, we observed the effect of the resonator's motion across the optical spot of the microscope. More precisely, with an autocorrelator optical setup, we observed the influence of the nanoresonator vibrations (625 kHz for the mechanical mode used in this experiment) on the collected photon statistics.

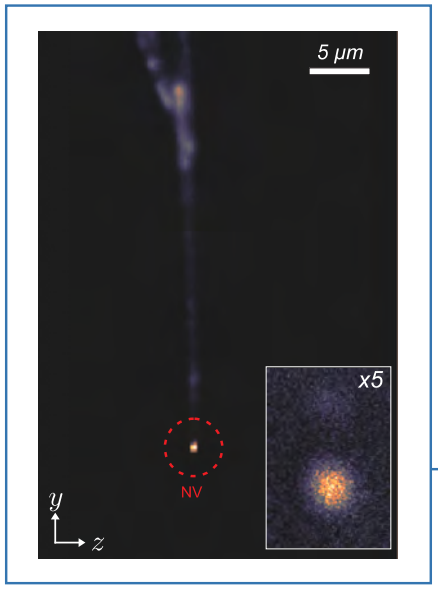

Figure 2 : Fluorescence map of the hybrid nano-resonator with a zoom onto the photon-emitting NV defect (red dashed circle) at its vibrating extremity.

Furthermore, the NV defect ground state is a spin triplet state with an ultralong coherence time that can be manipulated with microwave fields. We achieved magnetic coupling of the NV defect spin state to the oscillator's position via the combination of an external strong magnetic field gradient and the Zeeman splitting of the energy levels of the NV centre. More precisely, we immersed the system in a field gradient of 100 000 T/m (by approaching a structured permanent magnet). As the nanoresonator is set into motion, the NV centre sweeps through the magnetic field gradient, thereby experiencing large variations in the magnetic field. Thus, the energy levels of the NV centre, which depend on the magnetic field through the Zeeman effect, are subject to oscillations as well, and consequently are coupled to the nanoresonator motion.

The NV spin energy levels were probed by scanning a microwave field across the transition energy, while having the nano-resonator vibrating. By combining the microwave spectroscopy and a simultaneous optical read-out, a clear splitting in the spin energy spectrum, induced by the nano-motion, was observed in the fluorescence spectrum. In reverse, this coupling intrinsically generates a spin dependent force, whose magnitude is quantized and depends on the NV defect's spin state. This represents the key ingredient for mapping the quantum state of the spin onto the nanoresonator and thus creating non-classical states of motion. The possibility of generating spin-dependent forces combined with groundstate cooling of mechanical resonators will in the future allow us to perform quantum physics experiments with nano-mechanical oscillators.

CONTACTS

Olivier ARCIZET
olivier.arcizet@grenoble.cnrs.fr

Signe SEIDELIN
signe.seidelin@grenoble.cnrs.fr

FURTHER READING

A SINGLE NV DEFECT COUPLED TO A NANOMECHANICAL OSCILLATOR
O. Arcizet, V. Jacques, A. Siria, P. Poncharal, P. Vincent, and S. Seidelin
NATURE PHYSICS, 7, 879 (2011).

Screening in insulating granular aluminium films

Insulating granular aluminium films are experimental realizations of disordered insulators. They have received a renewed interest recently because they display slow relaxation of the conductance after a rapid-cool down to low temperature. This relaxation could be the experimental signature of a new type of glass predicted theoretically 30 years ago and called the electron glass. Measuring electrical field effects in thin films, we have found that part of the conductance relaxation is insensitive to gate voltage changes. This shows the existence of a metallic-like screening in the films and allows us to estimate the typical screening length. Although the nature of the screening is related to the existence of an electron glass, it has so far rarely been considered experimentally and theoretically.

Glasses are systems with such a slow internal dynamics that they cannot reach their thermodynamic equilibrium within any experimentally accessible time. Famous examples in condensed matter are structural and spin glasses. It was theoretically suggested in the 1980's, that the electrons can "freeze" at low temperature in disordered insulators (Anderson insulators) due to the coexistence of disorder and ill-screened electron-electron interactions. In these materials, the electrons move at low temperature from one localized site to another by thermally activated tunnelling, giving a "hopping" conductivity. The presence of interactions puts additional constraints on the electrons' motion: it favours simultaneous hops of many electrons, which can be extremely slow compared to individual jumps.

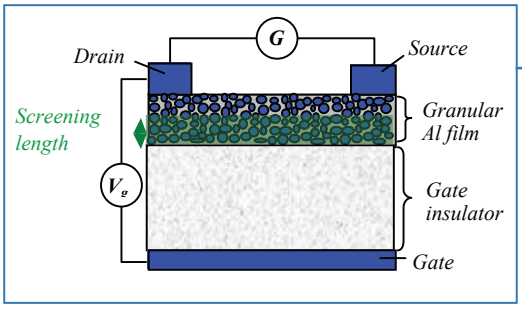

Figure 1: Schematic drawing of a MOSFET device. The part of the granular Al film in green is located at a distance less than the screening length from the gate insulator and is therefore sensitive to changes in the gate voltage Vg.

A fundamental question is whether electron glass features can indeed be observed experimentally in real systems. Interestingly enough, very slow conductance relaxations are found at low temperature in some disordered insulating systems, such as oxygen deficient indium oxide, granular aluminium or ultrathin films of metals. Following a rapid cool-down (quench), the conductance is seen to decrease as a logarithm of time, without any sign of saturation after weeks of measurement. Within the electron glass picture, this decrease reflects the approach of the electronic system towards its new, low temperature equilibrium (this will, in theory, require an infinite time).

Electrical field effect measurements have turned out to be a powerful technique for studying these slow relaxations. When disordered insulators are used as the (weakly) conducting channel of a MOSFET device (see Fig. 1), a gate voltage change can be used to inject or remove electrons, pushing the electronic system out of equilibrium.

We have recently shown how such MOSFET devices can also be used to determine the effective screening length of a disordered insulator like granular aluminium. Our insulating granular aluminium films are made of nanometric size aluminium grains embedded in an alumina matrix. We found that after a quench to 4K, only the part of the film closer than about 10 nm to the gate insulator (layer in green in Fig. 1) can be pushed out of equilibrium by a gate voltage pulse. The rest of the film continues its slow relaxation towards equilibrium, characterized by a logarithmic time decrease of the conductance, independently of the gate voltage values. This result, illustrated in Fig. 2 for a 20 nm thick film, clearly demonstrates the existence of a metallic-like screening length of about 10nm at 4K in our films.

Our observations address the important but little explored question of the screening in a disordered insulator. Electron glass models are generally developed in the limit of strongly localized electrons. But in real systems, there is a mobility of the charge carriers at finite temperature which gives rise to a metallic-like screening. It is believed that fast single electron processes establish a short-time screening length whereas multi-electron hops may lead to a slow decrease of this screening length as a function of time. Our results indicate how this screening length can be measured in real systems and they make it possible to determine its temperature and time dependence.

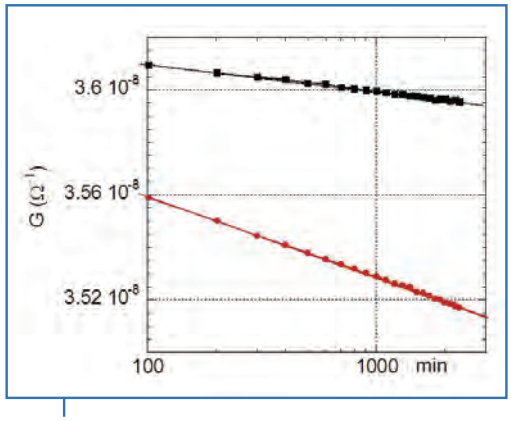

Figure 2: Conductance G of a 20nm thick granular aluminium film as a function of time (log scale) following a quench to 4.2K (Note the low values of G.). The red curve was measured with constant gate voltage Vg = 0V and represents the relaxation of the whole film. For the black curve, Vg was maintained most of the time at Vg=0, but the conductance was measured during short pulses to gate voltage Vg= -10V. Each pulse restores (re-excites) the part of the film sensitive to the gate field (green layer in Fig.1) to a constant state. Therefore, the black curve represents the sole relaxation of the part of the film beyond the screening length.

CONTACTS
Julien DELAHAYE
julien.delahaye@grenoble.cnrs.fr
Thierry GRENET
thierry.grenet@grenoble.cnrs.fr

FURTHER READING

SLOW CONDUCTANCE RELAXATION IN INSULATING GRANULAR ALUMINIUM: EVIDENCE FOR SCREENING EFFECTS
J. Delahaye, J. Honoré and T. Grenet
Phys. Rev. Lett. 106, 186602 (2011).

Precession Electron Diffraction for the structure solution of unknown crystalline phases

Following the discovery of X-rays by Roentgen, W. H. Bragg and W. L. Bragg used these waves to perform diffraction experiments on crystals and to determine the atomic positions within their ordered structures. X-ray crystallography has been hugely successful in elucidating the structures of minerals, metals and intermetallics, of biological molecules from small molecules to proteins and the DNA double helix. Later, neutron diffraction came in support of X-rays for detection of light elements or for distinguishing elements with similar atomic numbers. The importance of techniques to determine structure can be understood from the fact that knowledge of their structure is paramount to the understanding (and enhancement) of the properties of materials. Here we show the power of electron diffraction for structure solution in the case of nano-scale materials.

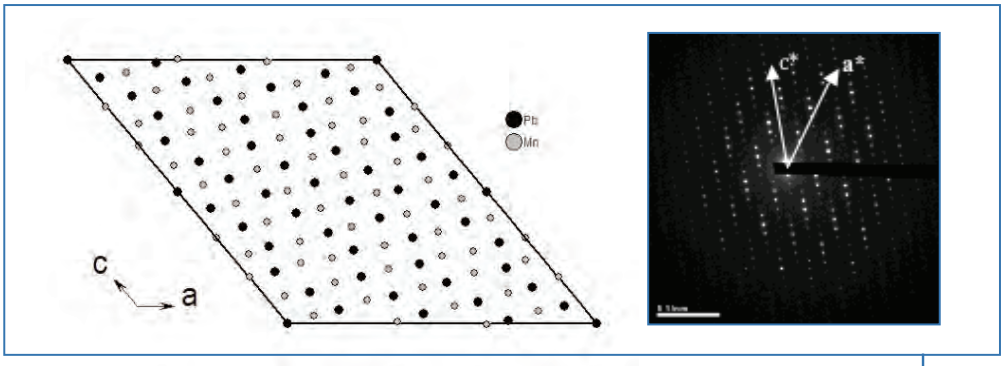

Figure: At left, projection of the cations of PbMnO2.75. At right: Precession Electron Diffraction pattern. The PED data allowed us to obtain all 29 independent cation positions.

Electrons, though they have been used for diffraction experiments in a transmission electron microscope (TEM) since 1933, have for a long time been regarded as inadequate for the solution of unknown crystal structures. This is linked to the strong interaction of electrons with matter. The approximation (routinely done for X-rays and neutrons) that a particle is scattered only once inside the crystal is no longer true for electrons. Even in the thinnest samples, many electrons undergo multiple diffraction. As a result it is extremely difficult to extract from the diffracted intensities meaningful values of the crystal "Structure Factors" used in the procedure for solving a crystal structure.

On the other hand, the strong interaction of electrons with matter is an asset when we study nano-particles. In these cases, X-ray diffracted intensities are very weak, inhibiting structure solution, while electrons are still diffracted to a considerable extent. X-ray diffraction then remains possible on powder samples, but this only yields the mean information for the sample. In the case of powders containing several different crystalline phases, this is insufficient for structure solution. It is therefore interesting to find a way to use electron diffraction for structure solution in the case of nano-structured materials.

The Precession Electron Diffraction (PED) technique, introduced in 1994, considerably relieves the problems linked to multiple diffraction. In this technique, a standard TEM is modified such that the electron beam can be tilted with respect to a crystallographic direction of the sample and precessed around a conical surface, having a common axis with the optical axis of the TEM. Even though PED reduces multiple scattering it does not eliminate it completely. Therefore, the crystallographic community has been very doubtful as to the real possibilities for solving structures by PED, even after the first successful solutions had been published.

In recent work we have studied systematically the influence of several parameters on the success of a structure solution from PED data. Our main result is that the number of measured reflections seems to be the most important parameter. To improve the chance of finding the structure solution, we need a high number of reflections, which in turn is determined by the number of zone axes accessible and the resolution that can be achieved in the reciprocal space. Surprisingly, the efficiency of this technique is not influenced by the precision of measuring the intensities of the reflections or the precision of extracting structure factors from these intensities, provided that strong reflections remain strong and weak reflections remain weak.

In order to test this hypothesis, we used experimental precession electron diffraction data that had previously been used for structure solution. We classified the reflections into just three categories: strong, medium and weak reflections. In each class we attributed the same intensity (the mean intensity of that class) to all reflections. We "deteriorated" the data in this way, for several different crystalline structures, going from simple to complex structures, structures showing low or high symmetry and crystals containing heavy or light elements or both. The structure solutions obtained from these voluntarily deteriorated data were (almost) as good as those obtained previously from the as-measured data. We still obtain the same accuracy of the cation positions; only the accuracy of the light atom positions is sometimes slightly reduced. The effects of multiple diffraction, which are the main hindrance to a precise determination of the structure factors in electron diffraction, are therefore no obstacle to structure solution.

In conclusion we have shown that the data quality obtained by Precession Electron Diffraction is quite sufficient to solve even complex structures in the case of nanometre sized particles. This technique will surely establish itself as an alternative to X-ray diffraction in the next few years.

CONTACT

Holger KLEIN
holger.klein@grenoble.cnrs.fr

FURTHER READING

PRECESSION ELECTRON DIFFRACTION OF MN2O3 AND PBMNO2.75: SOLVING STRUCTURES WHERE X-RAYS FAIL
H. Klein
Acta Cryst. A67, 303 (2011)

THE QUALITY OF PRECESSION ELECTRON DIFFRACTION DATA IS HIGHER THAN NECESSARY FOR STRUCTURE SOLUTION OF UNKNOWN CRYSTALLINE PHASES
H. Klein, J. David
Acta Cryst. A67, 297 (2011)

Probing complex magnetic configurations

Magnetic thin films and multilayers are investigated both for their fundamental magnetic properties and for spintronics (the coupling of magnetism with electronic transport). Reduced dimensionality and an increased role of the interfaces give new properties with potential applications in information and communication technologies. For such systems, X-ray Resonant Magnetic Reflectivity provides element-specific, chemical and magnetic interface profiles with sub-nanometer spatial resolution.

Much of the work on these systems is concerned with the coupling between two magnetic layers that are either in direct contact or separated by another layer. In general, they have "in-plane magnetic anisotropy", i.e. their axes of easy magnetization lie in the layer plane. There is also a strong interest in developing systems exhibiting perpendicular magnetic anisotropy (PMA) especially for high density magnetic storage. High stability of the magnetic state is sought for reliable storage and readout, but research aims also to reduce the energy needed to reverse the magnetization in the writing process. One way to achieve this is to realize a composite or hybrid structure, comprising layers with planar and perpendicular magnetization; the interlayer exchange coupling can ease magnetization reversals in the PMA layer. Optimizing such structures requires a detailed (i.e. layer resolved) and atomic-species selective picture of the non collinear magnetic configuration.

In collaboration with the Max Planck Institut, Halle, we have investigated the model layer system Fe_xCo_{1-x}/Rh/$Fe_{0.5}Co_{0.5}$ epitaxially grown on a Rhodium substrate. Here, the magnetic layers are separated by a nonmagnetic Rh layer. Alone, a $Fe_{0.5}Co_{0.5}$ layer exhibits perpendicular magnetization whereas an Fe layer (i.e. x=1) has an in-plane easy magnetization axis. Depending on the Rh separation-layer's thickness, the orientation of the magnetic moments may depart from the easy magnetization axis and/or from the direction of an external applied magnetic field.

We used X-ray Resonant Magnetic Reflectivity for characterizing the vertical profile of the in- and out-of-plane contributions of the Fe and Co magnetization in the thin film structure. As shown in inset in Fig. (a), a monochromatic, circularly polarized, X-ray beam is incident on the sample surface at an angle θ, and the reflected X-rays are detected at an emerging angle θ. The photon energy is chosen in the vicinity of the Fe or the Co L_3 absorption edge, to benefit from the difference in the X-Ray scattering process related to the magnetization of the specific atom. Their L_3 thresholds lie in the soft X-ray range and the long wavelengths allow measuring the reflectivity at large angles of incidence, which is favorable for probing the out-of-plane magnetic components. We measure the θ dependent intensities of right and left circularly polarized beams (Ip and Im in Fig. (a)). The magnetic asymmetry (Figs (b,c)), i.e. the normalized difference of the two scans (Ip-Im)/(Ip+Im), is related to the magnetization profile.

First, we studied two systems exhibiting out-of-plane magnetization in the two FeCo layers (Fig. (b)). The magnetic asymmetry is close to zero at small angles and becomes strong at large angles. The two different Rh layer thicknesses produce parallel/antiparallel magnetic alignments. Fig. (b) shows the sensitivity of the magnetic asymmetry to reversal of the magnetization in the upper layer, illustrated by an opposite sign for the two magnetic configurations at around 40°.

Second, we studied a system with a Fe layer instead of a FeCo layer (Fig. (c)). We demonstrated that one can distinguish the net in-plane and out-of-plane components of the magnetization by using different acquisition modes. The analysis of the magnetic asymmetry due to in-plane magnetization revealed that the FeCo layer had an in-plane component, indicating its magnetization was now slightly tilted. Furthermore, the analysis of the asymmetry related to the out-of-plane magnetization showed that the Fe layer's magnetism, normally in-plane, had an out-of-plane component. These effects result from the interlayer coupling. The asymmetry displayed in Fig. (c) is sensitive to both components (signal at both small and large angles). The vertical magnetization profile from this study is presented schematically (oriented arrows) in Fig. (c).

These measurements were done using an experimental device developed at the Néel Institute which is, to date, the only one which allows the investigation of a depth-resolved, out-of-plane magnetic profile.

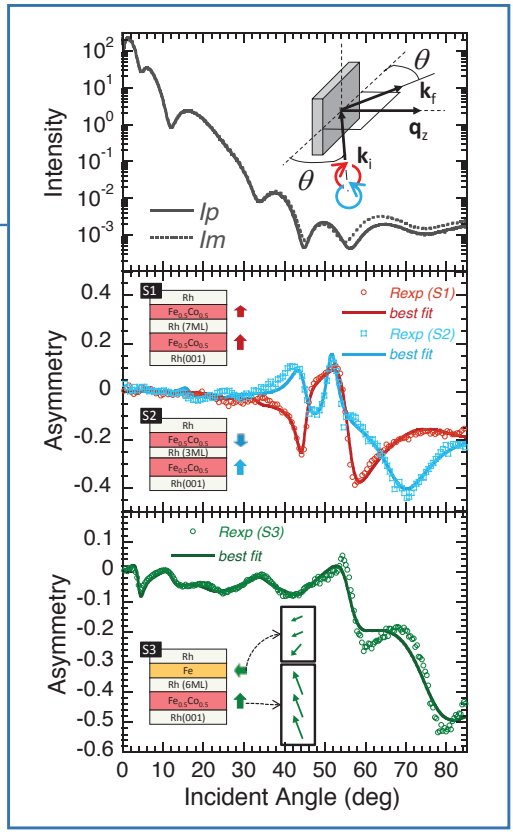

Figure: a) Reflected intensities Ip, Im (right and left circular polarizations) for 705.2 eV X-Rays (Fe L_3 edge) incident on FeCo/Rh(7 atomic monolayers)/ FeCo sample S1; the geometry of the X-Ray experiment is shown at right. b): Magnetic asymmetry (Ip-Im) /(Ip+Im) at 705.2 eV for samples S1 and S2. c) Magnetic asymmetry at 705.2 eV for sample S3; the sketch shows distribution of the Fe magnetic moments in the two magnetic layers; thickness of each slice= 0.3-0.4 nm.

CONTACT
Jean-Marc TONNERRE
jean-marc.tonnerre@grenoble.cnrs.fr

FURTHER READING

DIRECT IN-DEPTH DETERMINATION OF A COMPLEX MAGNETIC CONFIGURATION IN AN EXCHANGE-COUPLED BILAYER WITH PERPENDICULAR AND IN-PLANE ANISOTROPY
J.-M. Tonnerre, M. Przybylski, M. Ragheb, F. Yildiz, H. C. N. Tolentino, L. Ortega and J. Kirschner
Phys. Rev. B 84, 100407(R) (2011).

see also J. App. Phys. 111, 07C103 (2012)

6 HIGHLIGHTS 2012

Institut NÉEL
25, rue des Martyrs
B.P. 166
38042 Grenoble Cedex 9

neel.cnrs.fr